

CropSuite v1.0 - A comprehensive open-source crop suitability model considering climate variability for climate impact assessment

F. Zabel¹, M. Knüttel¹, B. Poschlod²

¹Department of Environmental Sciences, University of Basel, 4056 Basel, Switzerland

²Center for Earth System Research and Sustainability, Universität Hamburg, 20144 Hamburg, Germany

Correspondence to: florian.zabel@unibas.ch

Abstract.

Increasing demand for agricultural land resources and changing climate conditions require for strategic land-use planning and the development of adaptation strategies. Therefore, information about the suitability of agricultural land is a ~~necessary~~ prerequisite. Current suitability approaches often focus on single crops, can only be applied regionally and usually neglect the impact of climate variability on crop suitability. Here, we introduce CropSuite, a new comprehensive and easy-to-use ~~open-source~~ crop suitability model that ~~makes it possible~~ allows to overcome these shortcomings. ~~CropSuite uses a fuzzy logic approach and is based on the assumption of Liebig's law of the minimum. It provides a graphical user interface (GUI) and a wide range of pre- and postprocessing options, including a tool for data analysis, which allows users to easily apply the model and analyze the results. Further, it~~ includes a spatial downscaling approach for climate data, which ~~allows for performing~~ enables crop suitability analysis at very high spatial resolution. ~~CropSuite uses a fuzzy logic approach and is based on the assumption of Liebig's law of the minimum. Several~~ An expandable ~~number of environmental and socio-economic~~ factors that impact on crop suitability can flexibly be integrated into CropSuite by determining membership functions. CropSuite allows for the consideration of irrigated and rainfed agricultural systems, vernalization requirements for winter crops, lethal temperature thresholds, photoperiodic sensitivity and several other limitations ~~for crop growth~~. The model ~~endogenously~~ calculates and outputs climate-, soil-, and crop suitability, the optimal sowing- ~~and harvest~~ dates, the potential for multiple cropping, the (most) limiting factor(s), as well as the recurrence rate of potential crop failures ~~according to the inter-annual climate variability~~. In this study, we apply CropSuite for 48 crops at a spatial resolution of 30 arc seconds (1 km at the equator) for Africa. Thereby, we consider regionally important staple and cash crops ~~that are usually understudied~~, such as coffee, cassava, banana, oil palm, cocoa, cowpea, groundnuts, mango, millet, papaya, rubber, sesame, sorghum, sugar cane, tobacco, and yams. We find that the consideration of climate variability for calculating crop suitability makes a significant difference

31 on suitable areas, but also affects optimal sowing dates, and multiple cropping potentials. The most vulnerable regions
32 for climate variability are identified in Somalia, Kenya, Ethiopia, South Africa, and the Maghreb countries. The results
33 provide valuable crop-specific information that can be further used for climate impact assessments, adaptation and land-
34 use planning at global, regional, or local scale. CropSuite is provided open source and could be of interest for model
35 developers, scientists, and a wide range of potential users and stakeholders, such as farmers, companies, GOs, and NGOs.

36

37 **Key Words: Agriculture, Africa, Optimal Sowing Dates, Multiple Cropping, Maize**

38 **1 Introduction**

39 Climate change poses major challenges for agricultural production and food security. With warming climate, agricultural
40 suitability changes and suitable areas shift towards higher latitudes (Franke et al., 2021; Zabel et al., 2014). Crop
41 suitability models allow for a quantitative evaluation of land for crop cultivation and can therefore assess how the
42 suitability of land changes with changing climate. Contrary to mechanistic crop models (Jägermeyr et al., 2021;
43 Jägermeyr et al., 2020; Müller et al., 2024), crop suitability models are based on empirical approaches but are less
44 computational intensive and thus allow for the consideration of more crops at higher spatial resolution (Zabel et al., 2014).

45 ThereforeAs a result, crop suitability models provide important insights for sustainable land-use planning and climate
46 change adaptation, e.g. through cultivar change or land-use change. Akpoti et al. (2019) give an overview of existing
47 crop suitability approaches. Most studies are applied at regional scale (Maleki et al., 2017; Bonfante et al., 2015; Ranjitkar
48 et al., 2016), while just a few global approaches exist (Akpoti et al., 2019). In addition, Mmost studies focus just on single
49 crops and do not cover a variety of different crops (Ramirez-Villegas et al., 2013; Akpoti et al., 2020). Particularly for
50 Africa, domestically consumed staple crops, such as yams and cassava are often overseen in current studies, due to minor
51 economic relevance, despite their regional importance for food security (Chapman et al., 2020; Chemura et al., 2024;
52 Van Zonneveld et al., 2023; Karl et al., 2024). So far, none of the existing approaches systematically considers the impact
53 of climate variability on crop suitability, which is a major shortcoming, since climate variability is expected to increase
54 with climate warming and has a strong impact on agriculture (Vogel et al., 2019; Goulart et al., 2021; Ipcc, 2021).

55 The aim of this study is to introduce the CropSuite model, which is based on the crop suitability approach developed by
56 Zabel et al. (2014) and has continuously been further developed by Cronin et al. (2020) and Schneider et al. (2022a). The
57 model has previously been applied globally for 23 crops for different climate scenarios (Zabel, 2022). The model applies
58 Liebig's law of the minimum, assuming that the scarcest resource limits the crop growth, andCropSuite is based on a
59 fuzzy logic approach where, in contrast to Boolean logic, the truth value of variables can be any real number between 0
60 and 1. In fuzzy logic, fuzzy sets consist of elements whose degrees of memberships are described by membership
61 functions (Zadeh L.A., 1965). In our approach, we apply fuzzy logic to create, which uses crop-specific membership
62 functions (Fig. 1) describing the abiotic crop requirements between 0 (not suitable) and 100 (highly suitable) according

63 to various climatic, soil, and topographic variables (Zabel et al., 2014). This approach is adopted, fundamentally
 64 redesigned and expanded with the goal to provide a comprehensive but easy-to-use and flexible open-source model that
 65 can be applied e.g. by scientists, farmers, companies, national or international institutions, GOs, or and NGOs. Therefore,
 66 CropSuite is now completely reprogrammed in Python and consists of a graphical user interface (GUI), as well as several
 67 pre-processing and analysis tools, e.g. for selecting a simulation domain, statistically downscaling the climate data,
 68 interpolating the membership functions and automatically analyzing and mapping the results. In addition, CropSuite is
 69 complemented with a new approach to consider the impact of climate variability on crop suitability. It includes a user
 70 manual, which is provided together with the source code (Knüttel and Zabel, 2024).

71 2 Methods and Data

72 For this study, we apply CropSuite for Africa at 30 arc seconds spatial resolution (approximately 1 km² at the equator)
 73 with the goal to simulate relevant but often overseen crops for this continent (Van Zonneveld et al., 2023). Table 1 shows
 74 the 48 crops, that have been parameterized and simulated with CropSuite.

75
 76 **Table 1: List of 48 considered crops simulated with CropSuite.** Binomial names are given in brackets.

1. Alfalfa (<i>Medicago sativa</i>)	25. Olive (<i>Olea europacae</i>)
2. Arabica Coffee (<i>Coffea arabica</i>)	26. Onion (<i>Allium cepa</i>)
3. Avocado (<i>Persea americana</i>)	27. Papaya (<i>Carica papaya</i>)
4. Banana (<i>Musa spp.</i>)	28. Pea (<i>Pisum sativum</i>)
5. Barley (<i>Hordeum vulgare</i>)	29. Pineapple (<i>Ananas comosus</i>)
6. Beans (<i>Phaseolus vulgaris</i>)	30. Potato (<i>Solanum tuberosum</i>)
7. Cabbage (<i>Brassica oleracca</i>)	31. Rapeseed (<i>Brassica napus</i>)
8. Carrot (<i>Daucus carota</i>)	32. Rice (<i>Oryza sativa</i>)
9. Cashew (<i>Anacardium occidentale</i>)	33. Robusta Coffee (<i>Coffea canephora</i>)
10. Cassava (<i>Manihot esculenta</i>)	34. Rubber (<i>Hevea brasiliensis</i>)
11. Castor Bean (<i>Ricinus communis</i>)	35. Rye (<i>Secale cereale</i>)
12. Chickpea (<i>Cicer arietinum</i>)	36. Safflower (<i>Carthamus tinctorius</i>)
13. Citrus (<i>Citrus spp.</i>)	37. Sesame (<i>Sesamum indicum</i>)
14. Cocoa (<i>Theobroma cacao</i>)	38. Sorghum (<i>Sorghum bicolor</i>)
15. Coconut (<i>Cocos nucifera</i>)	39. Soy (<i>Glycine maximum</i>)
16. Cotton (<i>Gossypium hirsutum</i>)	40. Sugar Cane (<i>Saccharum officinarum</i>)
17. Cowpea (<i>Vigna unguiculata</i>)	41. Sunflower (<i>Helianthus annuus</i>)
18. Green Pepper (<i>Capsium annuum</i>)	42. Sweet Potato (<i>Ipomoea batatas</i>)
19. Groundnut (<i>Arachis hypogaea</i>)	43. Tea (<i>Camellia sinensis</i>)
20. Guava (<i>Psidium guajava</i>)	44. Tobacco (<i>Nicotiana tabacum</i>)
21. Maize (<i>Zea mais</i>)	45. Tomato (<i>Solanum lycopersicum esculentum</i>)
22. Mango (<i>Mangifera indica</i>)	46. Watermelon (<i>Colocynthis citrullus</i>)
23. Millet (<i>Pennisetum americanum</i>)	47. Wheat (<i>Triticum aestivum</i>)

77

78 We simulate a 20-year time period from 1991 to 2010 using the [Climate Hazards group Infrared Precipitation with](#)
 79 [Stations \(CHIRPS\) v2.0 daily data for precipitation](#) (Funk et al., 2015) and the [Climate Hazards Center Infrared](#)
 80 [Temperature with Stations \(CHIRTS\) v1.0 data for temperature](#) (Funk et al., 2019; Verdin et al., 2020) at 2.5 arc minutes
 81 [spatial resolution for Africa](#). Both data sets provide climatologies at daily to monthly resolution based on a combination
 82 [of satellite remote sensing and climate stations](#). They benefit from long-term geostationary satellite observations,
 83 [delivering consistent data since the 1980s at the quasi-global \(50°S-50°N\) scale](#).

84 In addition, soil and terrain information is required. Table 2 gives an overview of the soil and terrain data used for this
 85 study. Soil data is mainly based on [ISRIC SoilGrids](#) (Hengl et al., 2017), which has a spatial resolution of 250 m but is
 86 also provided at 1000 m spatial resolution. This data is reprojected to WGS84 and spatially interpolated using nearest
 87 neighbor to the spatial resolution of 30 arc seconds applied in this study. Base saturation, gypsum, and exchangeable
 88 sodium content (ESP, sodicity) are taken from the WISE database at a spatial resolution of 30 arc seconds (Batjes, 2016).
 89 For electric conductivity, the ISRIC Global Soil Salinity Map with a resolution of 250 m is used (Ivushkin et al., 2019).
 90 In contrast to the harmonized world soil database (HWSD) (Fao et al., 2012), the ISRIC soil datasets do not contain a
 91 layer for texture class. For this reason, the texture class is determined using the sand and clay layer of SoilGrids according
 92 to the United States Department of Agriculture (USDA) triangular diagram of soil texture classes (Fao et al., 2012). For
 93 soil depths greater than 200 cm up to 50 m, the ISRIC dataset on absolute depth to bedrock (Hengl et al., 2017) is
 94 complemented with the dataset from Pelletier et al. (2016), which covers soil depths up to 200 cm.

95 Available soil layers can be weighted in CropSuite as required. The SoilGrids datasets provide information for six depths:
 96 0-5 cm, 5-15 cm, 15-30 cm, 30-60 cm, 60-100 cm, and 100-200 cm (Hengl et al., 2017; Hengl et al., 2014). [According](#)
 97 [to Sys et al. \(1991\), soil properties have different effects on crop suitability depending on the soil layer. Accordingly, we](#)
 98 [use weighting factors as proposed by](#) ~~According to the available information, we adjust the different layers according to~~
 99 [the weighting factors \(see Table 2\) as suggested by](#) Sys et al. (1991) [\(see Table 2\). The different distribution of the soil](#)
 100 [depths between the SoilGrids data and the weighting factors by Sys et al. \(1991\) is taken into account by using a](#)
 101 [proportional weighting of the SoilGrids layers](#).

102 Terrain data are taken from the Shuttle Radar Topography Mission (SRTM) data set (Farr et al., 2007), which are used
 103 to calculate the slope at the applied spatial resolution. Please be aware that a coarser spatial resolution generally reduces
 104 the slope, which could result in an underestimation of possible slope limitations in mountainous regions. A possible
 105 terracing could remove the restriction due to the slope but usually terraces are too small to be considered at the aggregated
 106 spatial resolution of 30 arc seconds of the SRTM data in this study.

107

108 **Table 2: Soil and terrain data used in this study and the applied weighting of the different soil layers.**

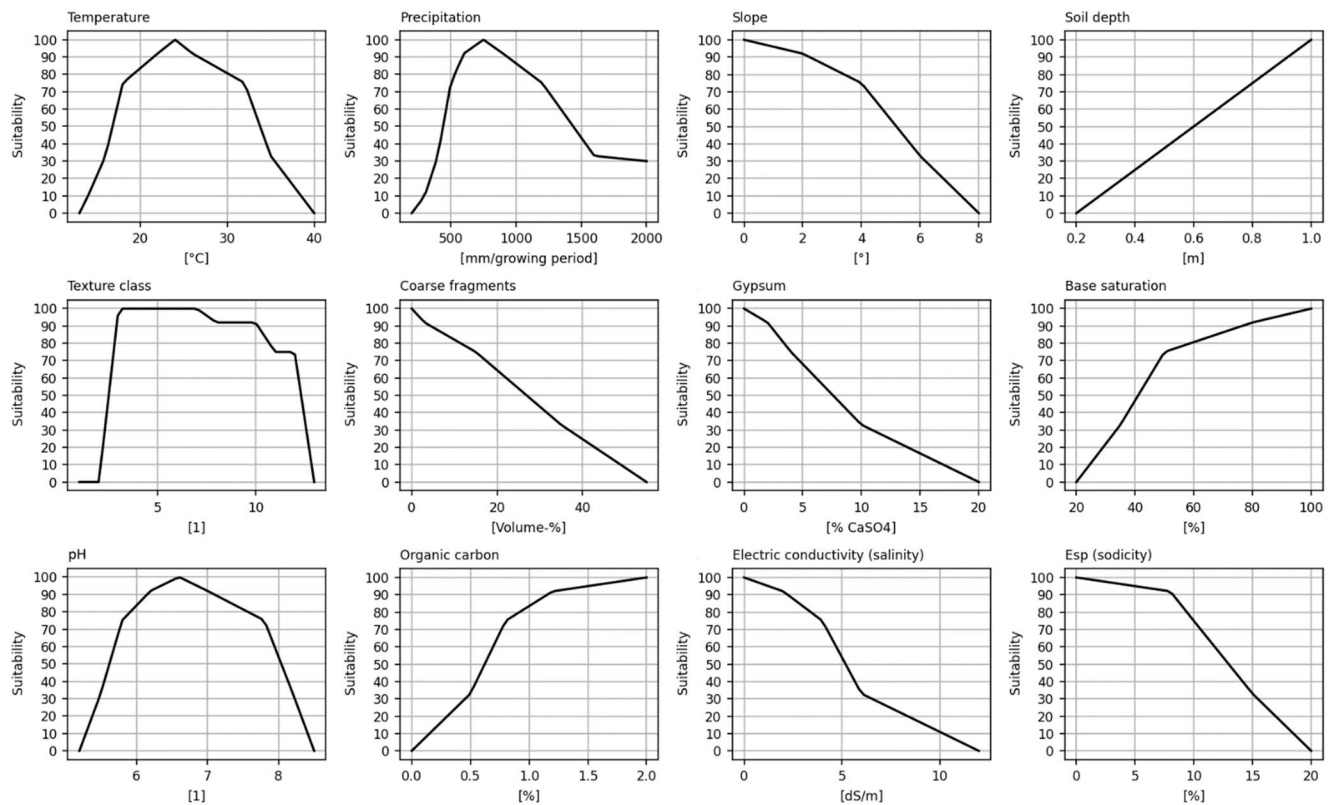
Parameter	Source	Weighting
-----------	--------	-----------

Base Saturation	ISRIC Harmonized Dataset of Derived Soil Properties for the World (WISE30sec)_(Batjes, 2016)	Only Top Soil
Coarse Fragments	ISRIC SoilGrids 250m_(Hengl et al., 2017)	0 - 25 cm: 2.0 25 - 50 cm: 1.5 50 - 75 cm: 1.0 75 - 100 cm: 0.75 100 - 125 cm: 0.5 125 - 150 cm: 0.25
Electric Conductivity	ISRIC Global Soil Salinity Map_(Ivushkin et al., 2019)	Only Top Soil
Gypsum Content	ISRIC Harmonized Dataset of Derived Soil Properties for the World (WISE30sec)_(Batjes, 2016)	Only Top Soil
Organic Carbon Content	ISRIC SoilGrids 250m_(Hengl et al., 2017)	0 - 25 cm: 2.0 25 - 50 cm: 1.5 50 - 75 cm: 1.0 75 - 100 cm: 0.75 100 - 125 cm: 0.5 125 - 150 cm: 0.25
Soil pH	ISRIC SoilGrids 250m_(Hengl et al., 2017)	0 - 5 cm: 0.33 5 - 15 cm: 0.33 15 - 30 cm: 0.33
Sodicity	ISRIC Harmonized Dataset of Derived Soil Properties for the World (WISE30sec)_(Batjes, 2016)	Only Top Soil
Soil Depth	ISRIC SoilGrids 2017 (Soil Depth <= 200 cm)_(Hengl et al., 2017) Pelletier et al. 2017 Pelletier et al. (2016) (Soil Depth > 200 cm)	No Weighting
Texture Class	Texture Class calculated from ISRIC SoilGrids s-250m Cclay and Ssand content (Hengl et al., 2017) according to USDA_(Fao et al., 2012)	0 - 25 cm: 2.0 25 - 50 cm: 1.5 50 - 75 cm: 1.0 75 - 100 cm: 0.75 100 - 125 cm: 0.5 125 - 150 cm: 0.25
Slope	SRTM aggregated to 30 arcsec_(Farr et al., 2007)	No Weighting

109

110 Membership functions for temperature, precipitation, slope, soil depth, texture class, coarse fragments, gypsum, base
111 saturation, pH, organic carbon, electric conductivity, sodicity (Fig. 1) are defined for the considered 48 crops relying on
112 information from Sys et al. (1993), which provide membership functions for most of the considered crops. Additionally,
113 data from the EcoCrop database, which provides crop [ecological](#) requirements for more than 2500 plant species
114 (Fao, 2024), is used for Cowpea, Rye, and Yams. CropSuite in principle allows the flexible addition of any further
115 membership function and dataset that is relevant [for the use case](#).

116 Nutrient deficits, such as nitrogen content are not considered in our approach, since according to our definition of crop
 117 suitability, they are not a decisive factor for the suitability of crops but rather depend on the crop management.
 118 Accordingly, we do not consider any soil tillage that can affect the soil properties, such as liming, which can influence
 119 the pH value.



120
 121 **Figure 1: Membership functions exemplarily for maize with a growing cycle of 110 days for considered climatic (mean temperature**
 122 **over the growing cycle, total precipitation over the growing cycle), topographic (slope), and soil constraints (soil depth, texture class,**
 123 **coarse fragments, gypsum, base saturation, pH, organic carbon, salinity, sodicity).**

124 Sys et al. (1993) uses a classification system with 6 classes, ranging from N2 as unsuitable to S0 as highly suitable. In
 125 this study, we dismiss the N1-classes due to a vague definition and differentiate three suitability classes, marginally,
 126 moderately, and highly suitable (Table 3).

127

128 **Table 3: Crop suitability classification system as used in this study compared to Sys et al. (1993).**

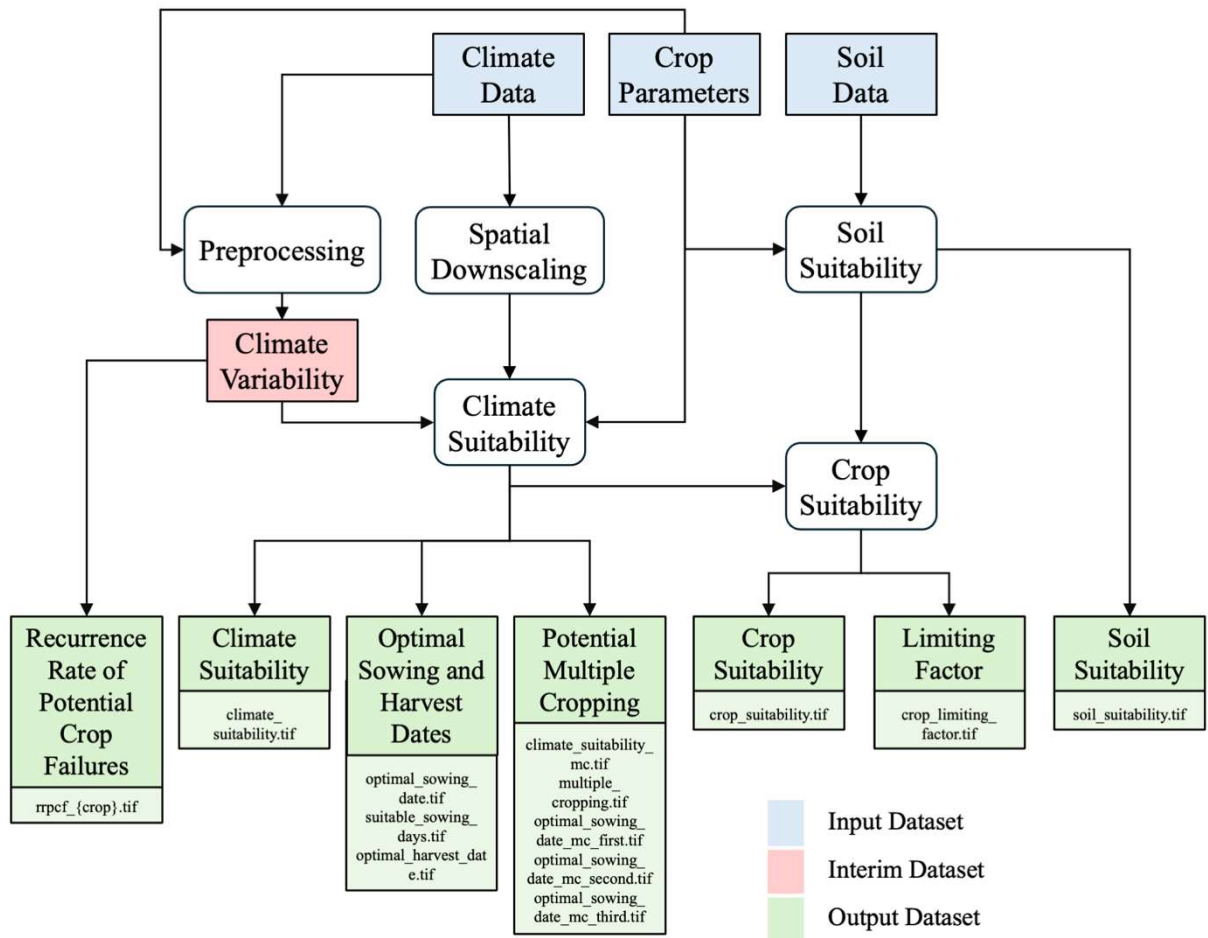
Suitability classes according to Sys et al.	Suitability range	Suitability classes used in this study
S0 (highly suitable)	100	75 – 100 (highly suitable)
S1 (very suitable)	80 – 99	
S2 (moderately suitable)	60 – 79	
S3 (marginally suitable)	40 – 59	1 – 32 (marginally suitable)
N1 (actually unsuitable and potentially suitable)	20 – 39	0 (unsuitable)
N2 (unsuitable)	0 - 19	

129 2.1 The CropSuite Model

130 Figure 2 shows the workflow and outputs of CropSuite, which first calculates a climate suitability (considering all climate
131 constraints) and then calculates a soil suitability (considering all soil and topography constraints). Both data records can
132 be output separately. Thereby, CropSuite applies Liebig's law of the minimum, for both the climate and the soil suitability
133 by choosing the lowest suitability value between the different soil parameters and climate variables respectively. Finally,
134 the crop suitability is calculated from the combination of both climate and soil suitability by again following Liebig's
135 law of the minimum, which means that the lowest suitability value between climate and soil suitability is chosen, since
136 it restricts overall crop suitability. The most limiting factor is identified as the parameter that imposes the greatest
137 constraint on growth for a specific crop. In addition, the magnitude of the constraint is output for each input factor.
138 Overall, CropSuite allows for a variety of outputs on optimal sowing- and harvest dates, suitable sowing days, multiple
139 cropping potentials, the limiting factor, and the recurrence rate of potential crop failures. [Output data format can be set
140 to GeoTIFF or NetCDF.](#)

141 CropSuite includes a pre-processing procedure which creates intermediate results for climate variability. Since climate
142 model data are usually available at relatively coarse spatial resolution, CropSuite has implemented a spatial downscaling
143 module for the climate data, which allows the model to be applied at very high spatial resolution from global to regional
144 to local scale. In this study, we apply a statistical downscaling to the climate data, refining the spatial resolution from 2.5
145 arc minutes to 30 arc seconds. In principle, the targeted spatial resolution can be set in CropSuite but is limited to the
146 available resolution of the additional input data, such as the soil data, whereas for the climate data, two different statistical
147 spatial downscaling methods are implemented requiring little computational effort. The first methodology is based on an
148 altitude regression for temperature (Marke et al., 2014), where the temperature gradients are extracted from the climate
149 model data itself via a moving window that can be set in size. Thereby, the extracted gradients must remain within the
150 natural boundaries for wet and dry adiabatic temperature gradients. The second downscaling methodology uses the
151 historical high-resolution spatial patterns for monthly temperature and precipitation taken from WorldClim at 30 arc
152 seconds spatial resolution (Fick and Hijmans, 2017). To downscale a coarse-resolution grid cell, all fine-resolution
153 WorldClim grid cells within the coarse-resolution cell are selected and aggregated per month. On this basis, additive
154 factors are calculated for temperature and multiplicative factors for precipitation separately for each month. Thereby the
155 sum (mean) of these additive (multiplicative) factors within the coarse-resolution cell amounts 0 (1). Considering the
156 monthly seasonality, these factors are applied to the coarse-resolution climate data, imprinting the spatial pattern of the
157 high-resolution reference data onto the coarse climate data [at daily time step](#). Both downscaling methods conserve mass
158 and energy from the climate input data by iteratively minimizing residuals over the simulation domain. For a more
159 advanced statistical downscaling to kilometer-scale, the expert user may apply more complex topographical downscaling
160 methods (Daly et al., 1994; Fiddes et al., 2022; Karger et al., 2023) or downscaling based on machine learning (Damiani
161 et al., 2024; Wang et al., 2021) outside of CropSuite. Furthermore, we do not recommend applying the implemented

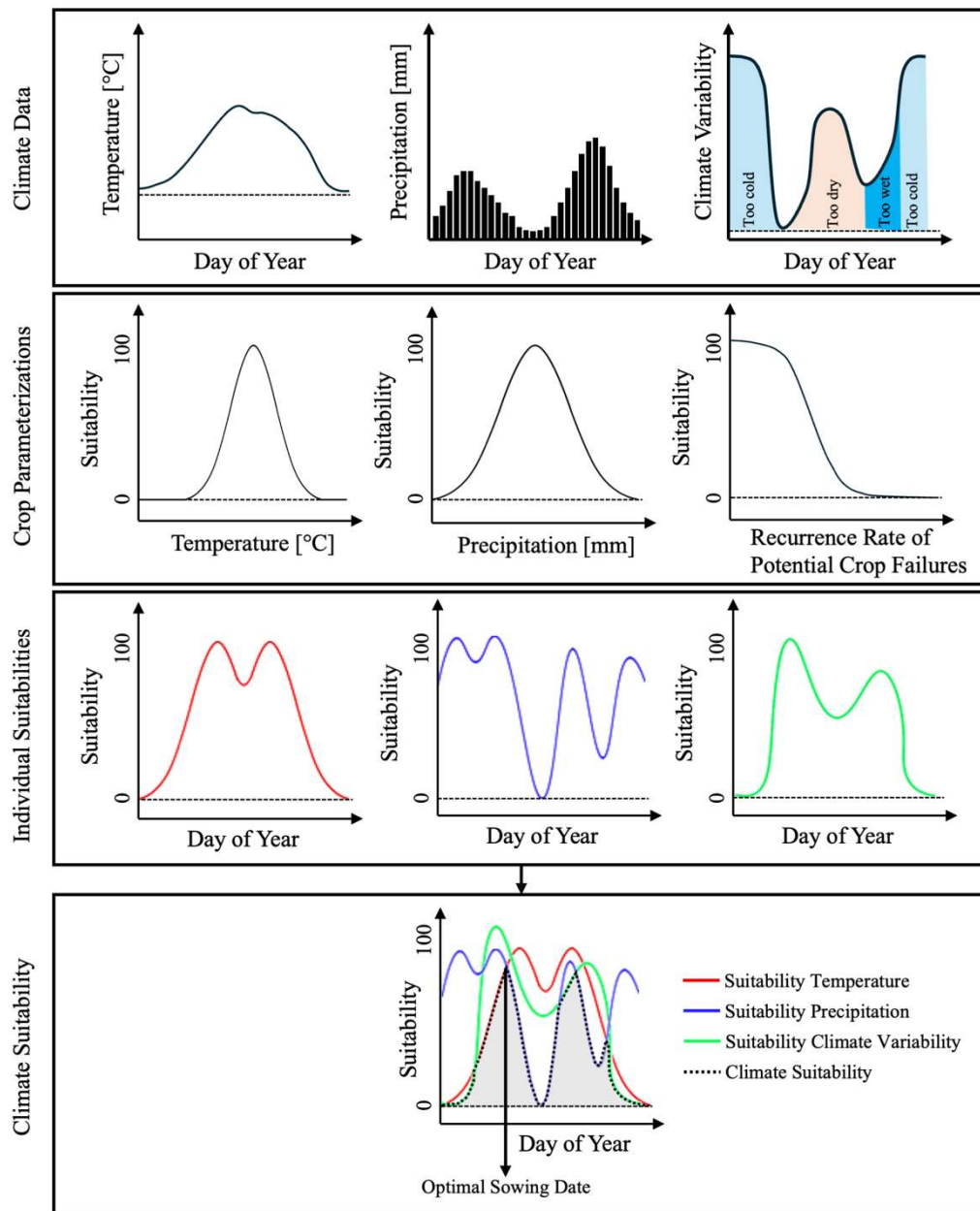
162 downscaling methods with high scaling factors from very coarse (hundreds of kilometers) to very high (single kilometer)
 163 resolution.



164
 165 **Figure 2: CropSuite workflow.** Input data in blue, intermediate results in red and output data in green. The processing steps are
 166 shown in white.

167 CropSuite requires daily climate data as an input for temperature and precipitation. As climate models tend to produce
 168 too many days with low-intensity precipitation called “drizzle bias” (Chen et al., 2021), days with aggregated daily
 169 precipitation values below 1 mm per day are considered to be dry days (Sun et al., 2006). This threshold can be set in the
 170 model. Both downscaled temperature and precipitation data and the calculated datasets for climate variability are used to
 171 calculate the climate suitability. Therefore, the crop-specific membership functions determine the suitability according
 172 to the average temperature, total precipitation and the recurrence rate of potential crop failures over the length of the
 173 growing cycle (time from sowing till maturity) for each day of year (DOY). Thereby, the suitability value for each DOY
 174 refers to the average conditions during the growing cycle from that DOY, which corresponds to the sowing date, until

175 maturity, determined by the length of the growing cycle which is set in the crop parameterization for each crop. For
176 perennial crops, the length of the growing cycle is set to 365 days. Climate suitability throughout the year is then identified
177 by selecting the minimum value (most limiting) of the three individual suitabilities for temperature, precipitation, and
178 climate variability. As shown in Fig. 3, the DOY with the highest climate suitability value over the year finally determines
179 DOY with the highest minimum of the three components throughout the year as shown in Fig. 3, thereby determining the
180 optimal sowing date for annual crops (optimal planting date for rice, which is not sown, but planted as a seedling in wet
181 rice cultivation). For perennial crops this is set to 1.



182
 183 **Figure 3: Schematic illustration of the determination of climate suitability, the optimal sowing date and the limiting factor.** The
 184 input data shows the annual course of temperature, precipitation and the recurrence rate of potential crop failure, indicating whether it
 185 is too cold, too dry, or too wet. The plant-crop parameterizations show the membership functions for either temperature, precipitation,
 186 and climate variability resulting in the individual suitability values for each DOY for either temperature (red line), precipitation (blue
 187 line), and climate variability (green line). Climate suitability throughout the year (black dashed line) results from the lowest of the
 188 three curves (most limiting) on any day. The highest value of climate suitability over the year finally determines the optimal sowing
 189 date. Finally, climate suitability and the optimal sowing date is determined by the highest minimum value of all three suitability curves.
 190 The limiting factor is the most constraining factor at this point.

191 For annual crops, CropSuite also calculates the potential for multiple harvests ~~of the same crop per year without~~
192 considering crop rotation. Between harvest and reseeded, we assume a certain time period (21 days in this study) for
193 field work and processing, which can be set flexibly in the model. Accordingly, all possible combinations of sowing dates
194 are tested with the aim to maximize climatic suitability to achieve the highest sum of climatic suitability within a year.
195 The optimal sowing dates are selected from the best sowing date combinations, resulting in one, two, or three sowing
196 dates per year. A multiple cropping layer is output that shows how often a crop can be harvested.

197 CropSuite distinguishes between rainfed and irrigated agricultural systems, which can be selected before starting the
198 simulation. For the irrigated case, precipitation is not considered as a constraining factor with consequences for all further
199 calculations, affecting e.g. the climate variability, the optimal sowing date, and the multiple cropping. For this study, we
200 separately simulated both, rainfed and irrigated options for all crops. In the post-processing, we combined both datasets
201 according to the irrigated areas dataset by Meier et al. (2018) (Fig. S1), which is available at 30 arc-seconds spatial
202 resolution.

203 For germination, crop-specific temperature and soil water ~~conditions~~ requirements can be set in the model. The latter can
204 be considered for rainfed conditions by defining a certain amount of precipitation within a certain period of time after
205 sowing.

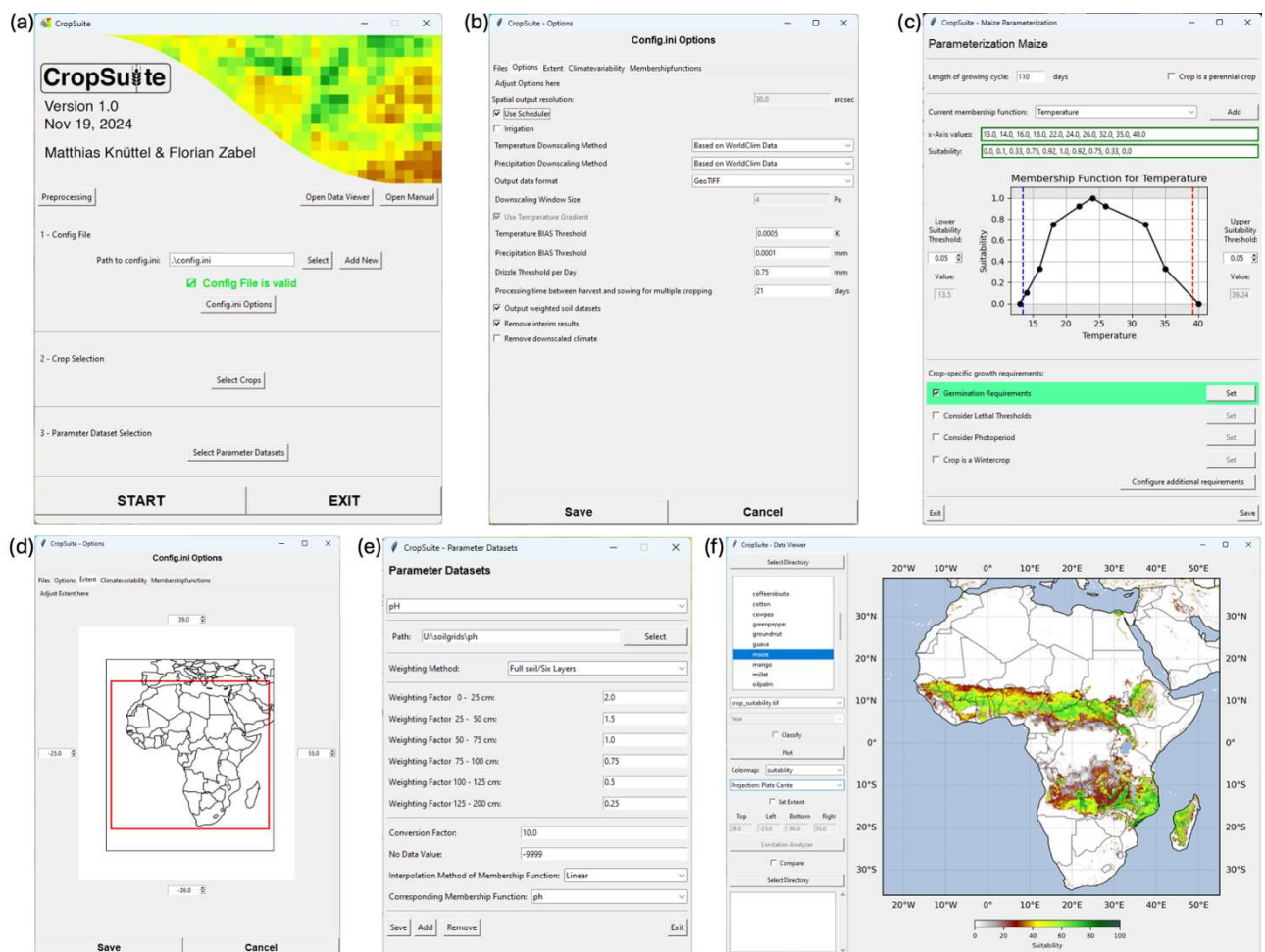
206 Some crops, such as soybean have a high photoperiodic sensitivity which can limit their suitability (Cober and Morrison,
207 2010; Abdulai et al., 2012). Therefore, crop-specific photoperiodic sensitivity can be considered in CropSuite by defining
208 a maximum and minimum day length in average over the growing cycle ~~can be considered in CropSuite~~.

209 Additional lethal climatic limitations ~~are~~ can be taken into account in CropSuite. We assume permafrost on areas with an
210 average annual temperature below 0° C, which is computed from the downscaled climate input data. A maximum lethal
211 temperature threshold of >40°C in average over the growing cycle is set for all crops (Asseng et al., 2021). In addition, a
212 minimum and maximum threshold for the lethal temperature over a certain consecutive number of days can be set in the
213 model crop-specifically. Further, the maximum number of consecutive dry days can be set dependent on the crop.

214 CropSuite allows for the consideration of vernalization requirements for winter crops. Therefore, crop-specific
215 temperature requirements with minimal and maximal temperature thresholds for a certain number of vernalization
216 effective days can be configured in the model. Accordingly, CropSuite simulates for each location, if and when these
217 vernalization requirements are fulfilled, which impacts on the length of the vernalization period and the optimal sowing
218 date. An offset of days from sowing to the start of the vernalization period can optionally be added.

219 A GUI is available for CropSuite that allows users to easily set-up the model, parameterize the crop requirements and the
220 membership functions (Fig. 4a-e), and to start the simulations. Further, new membership functions can be created, an
221 unlimited number of crop-specific requirements can be defined, and any additional data can be added, which can be
222 flexibly assigned to the defined membership functions (Fig. 4e). Moreover, new crops or crop varieties can be added.

223 The GUI also allows for the visualization, analysis and comparison of the results (Fig. 4f).



224
 225 **Figure 4: Graphical User Interface of CropSuite.** (a) shows the main screen, (b) exemplarily shows available model settings, (c)
 226 shows the available options for crop parameterizations exemplarily for maize, (d) shows the window to set-up the simulation domain,
 227 (e) exemplarily shows the set-up of a parameter dataset for soil pH, and (f) shows the integrated data viewer in CropSuite.

228 2.2 Climate Variability

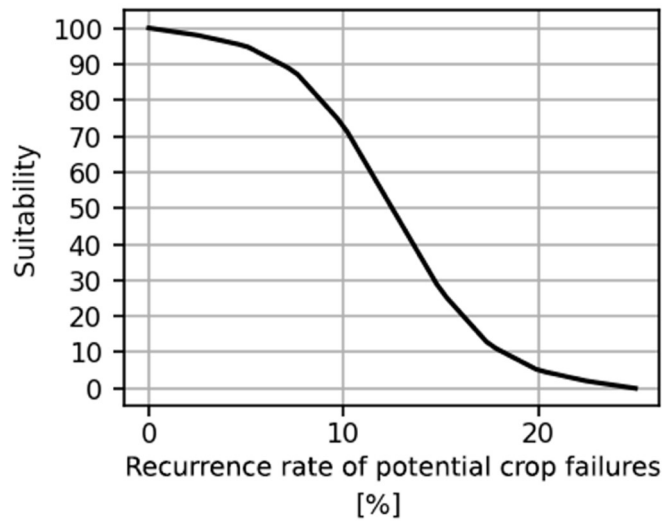
229 In addition to several improvements and redesigns, one of the most important advancements in CropSuite is the
 230 consideration of climate variability for the assessment of crop suitability. Usually, crop suitability models consider long-
 231 term climate averages, e.g. 10, 20 or 30-year periods and climatic trends that affect crop suitability (Ramirez-Villegas et
 232 al., 2013; Schneider et al., 2022b). They are not designed so simulate seasonal yields, as for instants mechanistic crop
 233 models do (Jägermeyr et al., 2021). However, existing crop suitability approaches may overestimate crop suitability when
 234 only long-term averages are considered, because a high climatic variability may result in a high frequency of unsuitable
 235 years, which would result in crop failures. This would however significantly increase the risk for farmers that require
 236 stable and plannable conditions. As a result, a farmer may conclude that the risk of crop failures due to unstable climate

237 conditions in a certain region is too high for being suitable for crop cultivation. As such, climate variability is not a purely
238 ecological limitation but depends on the socio-economic circumstances of how farmers deal with the risk of crop failure.
239 We developed an approach that allows for the consideration of climate variability, and thus the implicit integration of
240 socio-economic limitations in the suitability assessment of crops.

241 Therefore, we specify a crop-specific lower and upper threshold for temperature and precipitation. We recommend these
242 thresholds at-between the higher and lower 5th and 10th and the 90th and 95th percentile-suitability values of the crop-
243 specific membership function, respectively (Figs. 1, 4c). If the suitability of the membership function does not approach
244 0 at its high (low) limit, we recommend setting the threshold to the highest (lowest) value of the membership function.
245 This is the case for the wet limit of the precipitation membership function for maize (see Fig. 4c). For each year within a
246 given period of time (here we use 20-year time periods), it is tested and totaled, how often these thresholds exceed or fall
247 below during the growing cycle for all possible sowing dates (January 1st until December 31st). As a result, a variability
248 dataset is generated for each DOY, indicating the number of years in which at least either the temperature or the
249 precipitation exceeds or falls below the threshold values. The number of years is divided by the length of the time period
250 (here 20 years) to obtain the recurrence rate of potential crop failures. This data can be stored as a two-dimensional raster
251 file for perennial crops or as a three-dimensional raster file for non-perennial crops, with each of the 365 DOYs
252 representing the condition for the respective sowing day.

253 For rainfed agricultural systems, cases that are considered for climate variability include excessively high or low
254 temperatures and precipitation, while for irrigated agricultural systems, only excessively high or low temperatures and
255 excessively high precipitation are considered, to address potential water logging, plant diseases or root rotting. Due to
256 computational limitations, the preprocessing of the climate variability is carried out at the resolution of the input climate
257 data (2.5 arc minutes) and is further interpolated bilinearly to the output resolution of 30 arc seconds.

258 Finally, we introduce a membership function defining the impact of climate variability on crop suitability. As shown in
259 Fig. 5, a sigmoid is adopted for the course of the function. According to expert knowledge, we set this sigmoid function
260 in a way that it reduces suitability to 0 when the recurrence rate of potential crop failure is greater than once every 4 years
261 (25%). However, this function may be different in different parts of the world and different between crops (see
262 Discussion).



263

264

265

Figure 5: Membership function for climate variability showing the impact of the recurrence rate of potential crop failures on crop suitability. [The seasonal \$R_{recurrence}\$](#) recurrence rate is shown in percent.

266

3 Data-Comparison/Model evaluation

267

Crop suitability is difficult to validate or measure, nor is it equivalent to agricultural yields or production values. However, a comparison with other studies and data can provide valuable information and build confidence in the approach.

268

269

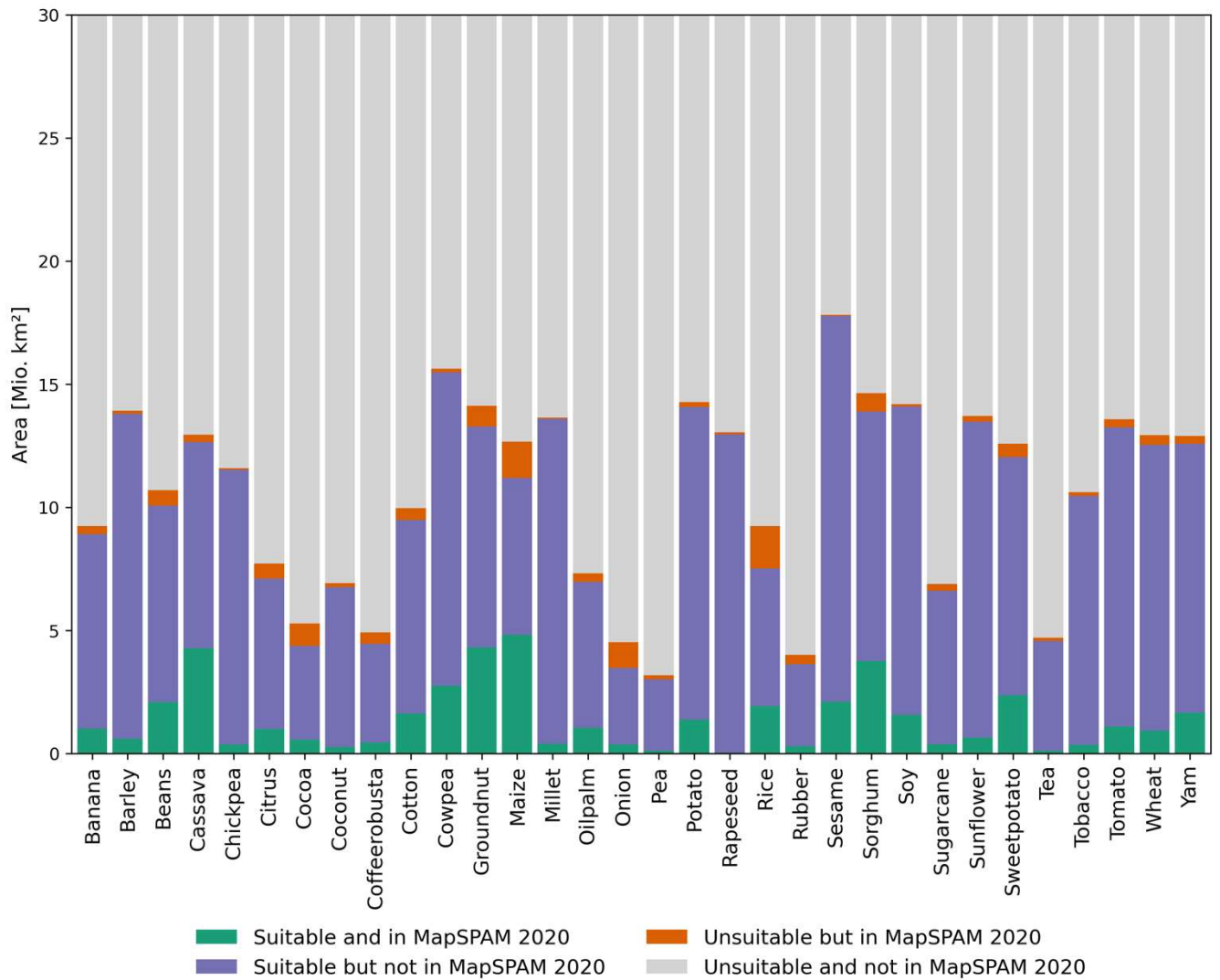
3.1 Comparison with Harvested Area

270

In principle, a crop should be suitable where it is already cultivated. ~~According to~~ [According to](#) this premise, we compare ~~the suitable area simulated with CropSuite with the harvested areas from the global spatially-disaggregated crop production statistics data for 2020 (MapSPAM 2020 v1.0) produced by the International Food Policy Research Institute (IFPRI) using the Spatial Production Allocation Model (SPAM) (Ifpri, 2024). MapSPAM 2020 (Ifpri, 2024) with the suitable area from our simulation~~ [The CropSuite results for Africa considering climate variability and are combined for irrigated and rainfed areas according to Meier et al. \(2018\)](#) ~~from our simulation results for Africa~~. While MapSPAM relates to the year 2020, our simulations refer to the ~~1990-2010~~ [1991-2010](#) time period, which could be a source of uncertainty. Nevertheless, we used MapSPAM 2020 ~~instead of other available versions of MapSPAM~~, since it includes 32 crops from our investigation ~~and is the latest released version of MapSPAM that was created with a special focus on Africa~~. [A comparison between CropSuite and different MapSPAM versions is shown exemplarily for maize in Fig. S32, revealing a considerably better fit with CropSuite in the MapSPAM 2020 version](#). For comparison, harvested areas below 10 ha per pixel are excluded from the calculation and the high spatial resolution of the CropSuite model output is resampled to the same spatial resolution (5 arc minutes) than the MapSPAM 2020 data.

282

283 Figure 6 depicts the results of this analysis for all crops, where green and ~~blue-purple~~ bars represent areas that are suitable,
284 while ~~red-orange~~ and green areas ~~indicate-represent~~ harvested areas in MapSPAM. ~~Purple bars indicate suitable areas that~~
285 ~~are currently not used by the respective crop.~~ While green areas are also identified as being suitable in our approach, ~~red~~
286 ~~orange~~ areas are ~~harvested areas according to MapSPAM but~~ not suitable ~~according to~~ CropSuite ~~despite the respective~~
287 ~~crop is harvested according to MapSPAM.~~ ~~Crops with the largest mismatching areas are rice, maize, and onion (Fig. 6).~~
288 ~~Considering the ratio of red to green areas in Fig. 6, m~~Most crops show a small proportion of ~~mismatch~~~~orange to green~~
289 ~~areas~~, except for onions, ~~rapeseed, cocoa, peariee~~, rubber, ~~eeoea, and tea~~, coffee, and rice (Fig. S23). This can have
290 various causes, such as data uncertainty of climate, soil and irrigation data (Avellan et al., 2012), incorrect membership
291 functions, the use of different crop varieties, or an incorrect localization of the cultivation areas in MapSPAM due to high
292 uncertainties in the underlying national statistical data, especially in African countries (Yu et al., 2020), or applied crop
293 management practices that could level out ecological limitations.



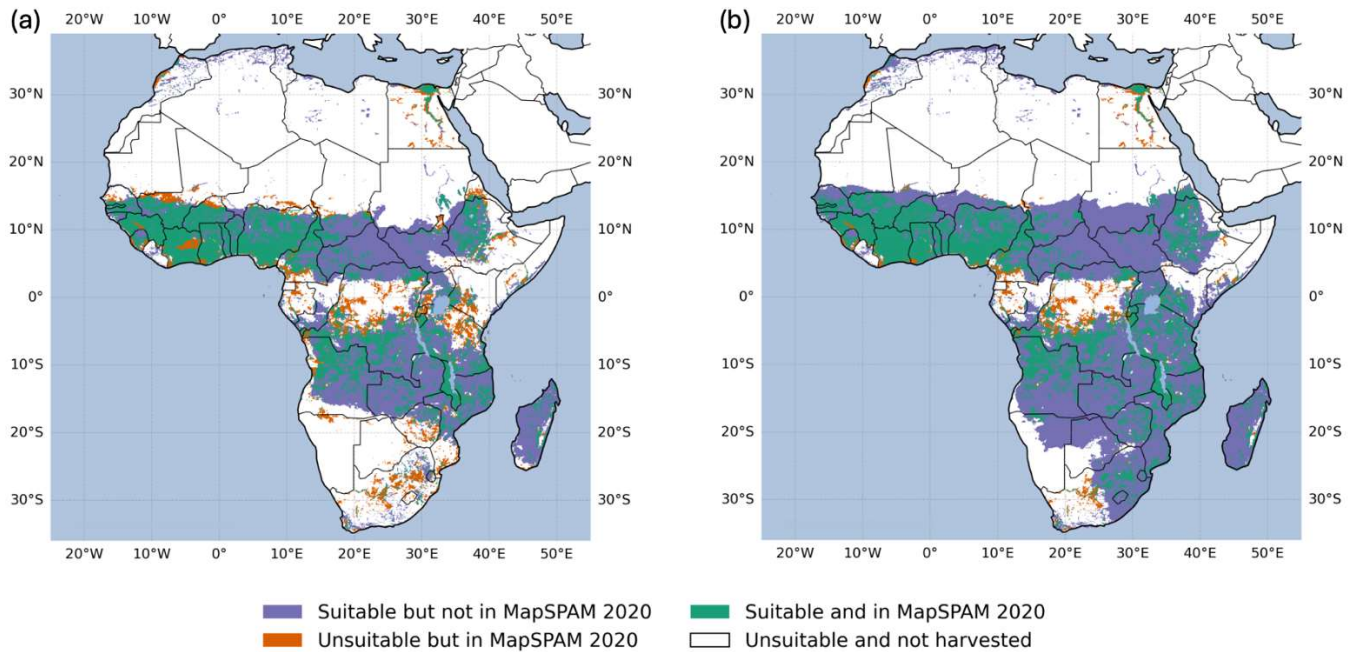
294

295 **Figure 6: Comparison of CropSuite with MapSPAM 2020 for all matching crops.** CropSuite results combine irrigated and rainfed
 296 areas according to Meier et al. (2018) and consider climate variability. Areas on which the respective crop is harvested according to
 297 MapSPAM and which are suitable according to CropSuite are shown in green, areas that are suitable but on which the crop is not
 298 harvested are shown in bluepurple. Areas that are not-unsuitable but are harvested according to MapSPAM are shown in redorange,
 299 while unsuitable areas that are not harvested according to MapSPAM are shown in gray.-

300 Figure 7a shows the spatial comparison between crop suitability and harvested areas for maize. Areas where maize is
 301 harvested according to MapSPAM, although CropSuite has identified these areas as unsuitable, are found mainly in
 302 Egypt, the northern Sahel, the Congo Basin, as well as parts of Cameroon, Gabon, Kenya, Tanzania, Zimbabwe and
 303 South Africa. Figure 7b shows the comparison ignoring the impact of climate variability on crop suitability. Disregarding
 304 climate variability results in large (blue) areas, which are considered suitable but are no harvest areas according to
 305 MapSPAM, especially along the dry belts (15°N and 20°S). Our approach considering climate variability (Fig. 7a)

306 reduces these blue areas, but induces some mismatches, where MapSPAM indicates harvested areas and CropSuite shows
 307 no suitability (red areas). We find that the mismatching areas along the dry belts (including the Sahel) and in eastern
 308 Africa (Tanzania, Kenya) are often associated with limits due to climate variability. This indicates that the thresholds for
 309 climate variability (section 2.2) and the membership function (Fig. 5) might be parameterized slightly too exclusive.
 310 However, some of these regions might be used as cropland by smallholders or subsistence farmers despite the high risk
 311 of crop failures.

312 While in the inner tropics, the reason for limited crop suitability can primarily be attributed to soil acidity (pH), indicating
 313 possible uncertainties with used SoilGrids dataset, differences in Egypt mainly result from discrepancies according to
 314 different assumptions on irrigated areas.



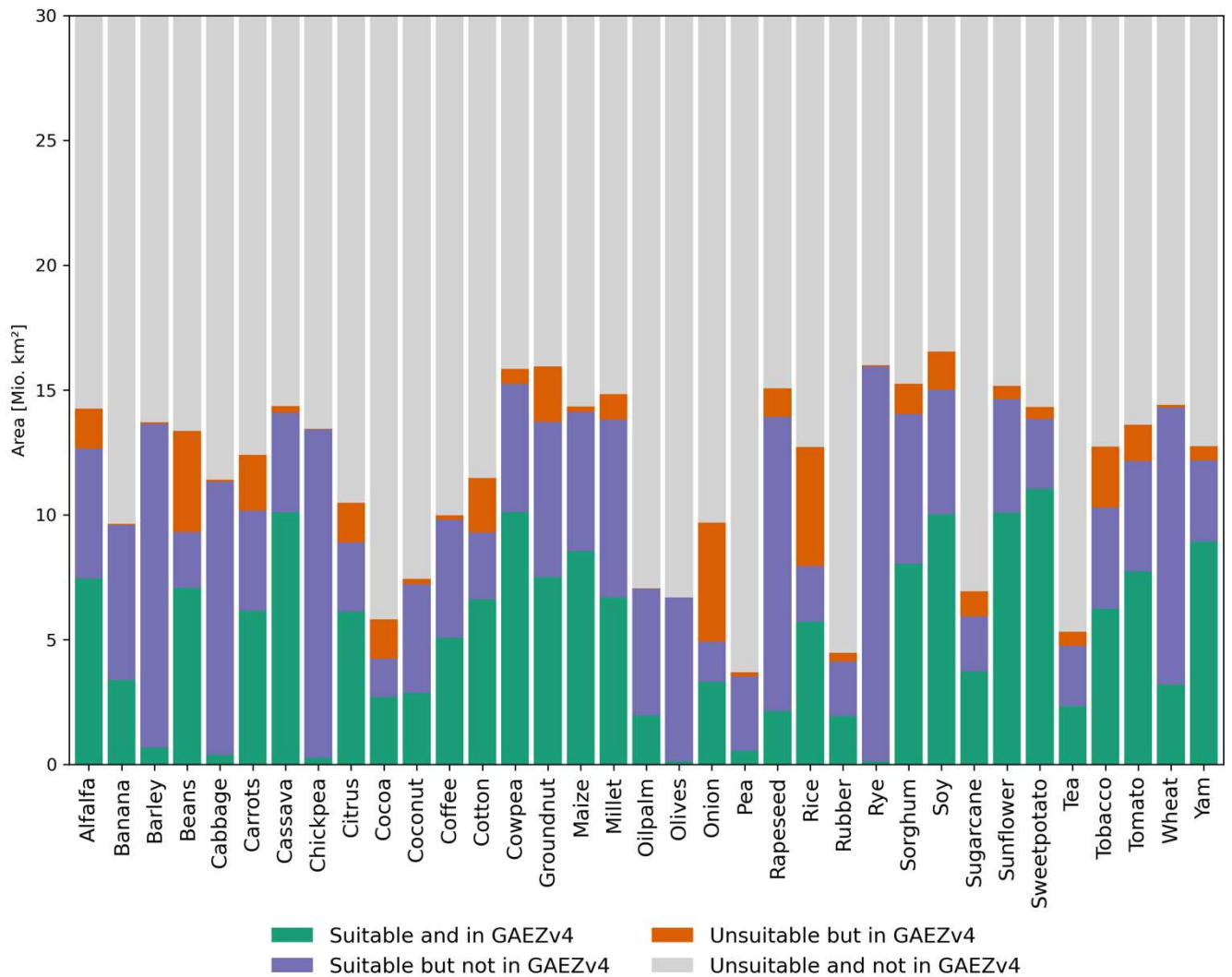
315
 316 **Figure 7: Comparison of CropSuite with MapSPAM 2020 for maize.** (a) shows the comparison with consideration of climate
 317 variability in CropSuite, while climate variability is not considered in (b). Areas on which the respective crop is harvested according
 318 to MapSPAM and which are suitable according to CropSuite are shown in green, areas that are suitable but on which the crop is not
 319 harvested are shown in blue. Areas that are not suitable but are harvested according to MapSPAM are shown in red. Unsuitable areas
 320 that are not harvested according to MapSPAM are shown in white. (a) shows the comparison with consideration of climate variability
 321 in CropSuite, while climate variability is not considered in (b).

322 3.2 Comparison with GAEZ

323 A state-of-the-art agroclimate-edaphic suitability assessment for crops is provided by the Global Agro-Ecological Zones
 324 (GAEZ) v4_ (Fischer et al., 2021). For comparison with CropSuite, the suitability range of the GAEZ data we used GAEZ
 325 data for the time period 1981-2010 for high input level, rainfed conditions and the option 'all land in grid cell'. The high
 326 input level refers to advanced management assumptions (fully mechanized, optimum application of nutrients and
 327 chemical pest, disease and weed control) (Fischer et al., 2021), which correspond best to the assumptions made in

328 CropSuite for this study. The suitability range of the GAEZ data is transformed to the classification system as shown in
329 Table 3. ~~In addition,~~ The CropSuite data for rainfed conditions is resampled (using the average) to the same spatial
330 resolution of 5 arc minutes than the GAEZ data. For this comparison, we use CropSuite data without climate variability,
331 since the GAEZ approach does not consider climate variability as well. Coffee was compared against the best type of
332 robusta and arabica, as done in the GAEZ data (Fischer et al., 2021).
333 Overall, there are large overlaps between the GAEZ and CropSuite (Fig. 8). Generally, CropSuite identifies larger suitable
334 areas than GAEZ for Africa (purple bar in Fig. 8), particularly for barley, cabbage, chickpea, rapeseed, rye and wheat. A
335 main reason for differences may be due to different underlying soil data, GAEZ uses the HWSO while CropSuite uses

336 the SoilGrids data. The consideration of climate variability in CropSuite mainly results in larger areas that are unsuitable
 337 in CropSuite but still suitable in GAEZv4 (orange bars) (Fig. S4).

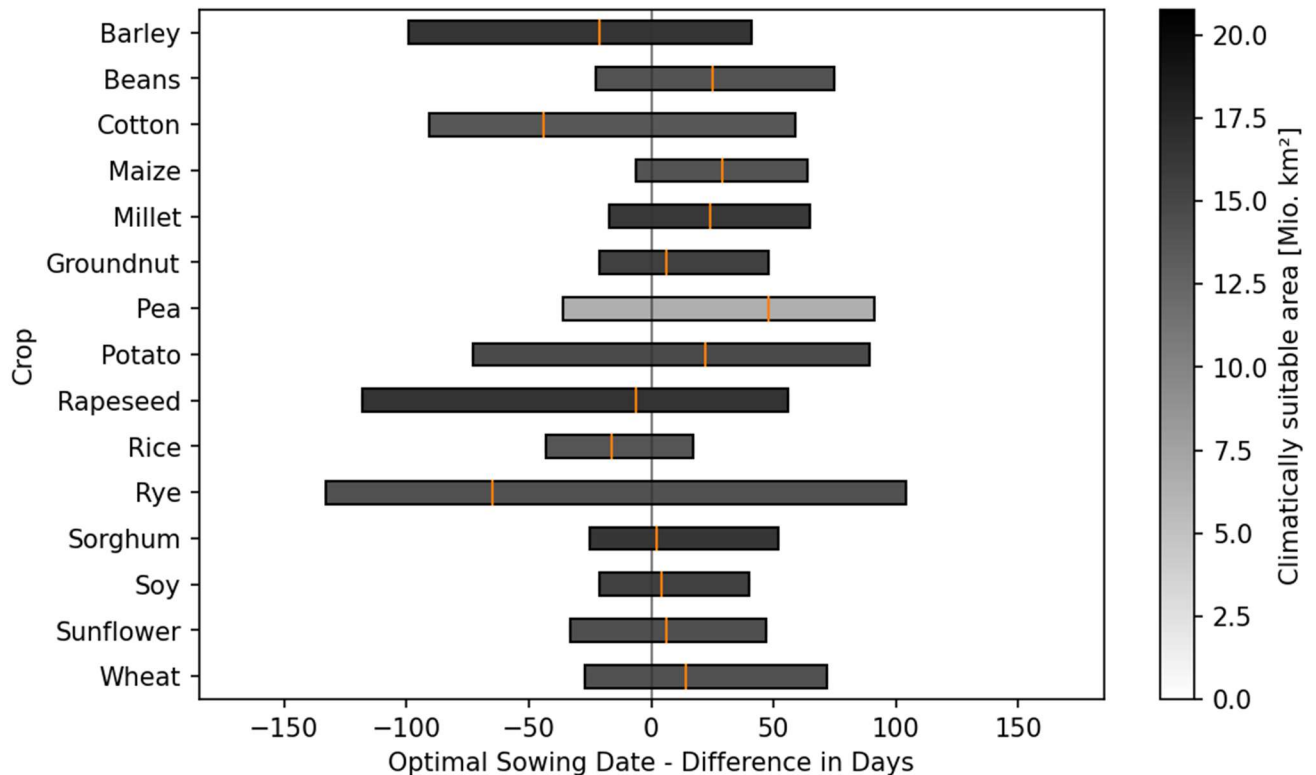


338
 339 **Figure 8: Comparison between CropSuite and GAEZv4 suitability data for all matching crops.** CropSuite results are shown
 340 without consideration of climate variability. Areas that are suitable in both data, CropSuite and GAEZv4 are shown in green, areas
 341 suitable in CropSuite but not suitable in GAEZv4 are shown in purple. Unsuitable area in CropSuite that is suitable in GAEZv4 is
 342 shown in orange. Areas that are unsuitable in both data are shown in gray.

343 3.3 Comparison of Optimal Sowing Dates with the GGCM Crop Calendar

344 Another method of validation involves comparing the optimal sowing dates computed with CropSuite with the ~~GGCM~~
 345 crop calendar from the Global Gridded Crop Model Intercomparison (GGCMI), which is available globally for a variety
 346 of different crops at half degree spatial resolution (Jägermeyr et al., 2021). Figure 9 illustrates the average differences of

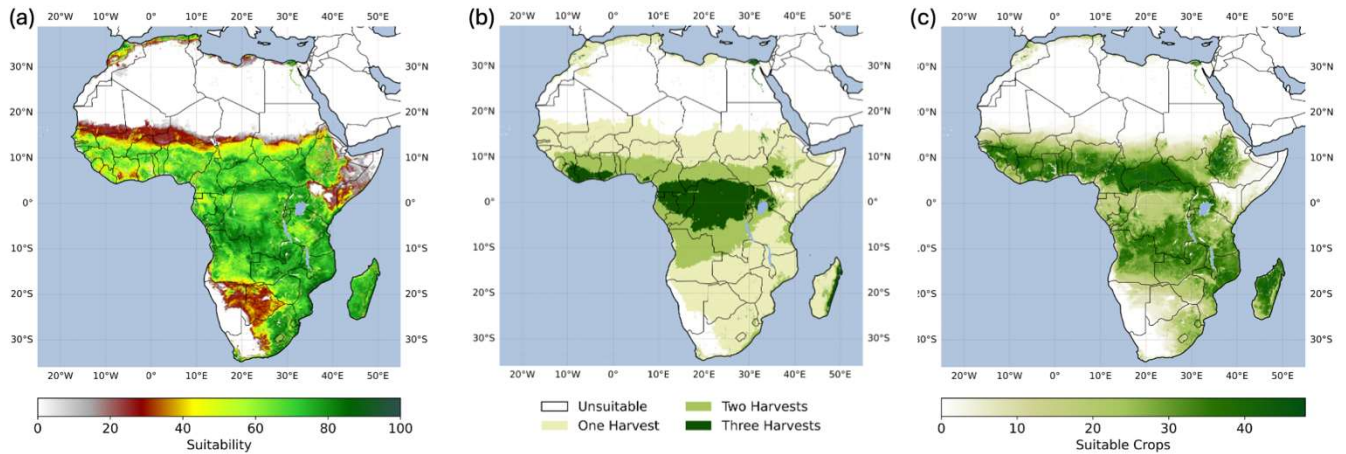
347 the sowing dates across Africa, averaged for the matching crops between the two datasets. The [analysis-comparison](#) is
 348 performed at a [spatial](#) resolution of 30 arc seconds (Fig. 9) and at half degree resolution (see Fig. S5). For the high spatial
 349 resolution, ~~the~~ GGCMI data are ~~bilinearly~~-interpolated to 30 arc seconds -using nearest neighbor-and then compared
 350 ~~with the CropSuite data~~. Unlike CropSuite, which displays the optimal sowing date, the GGCMI data show the actual
 351 sowing date based on ~~interpolated-extrapolated~~ statistics. Thus, there might be differences between the optimal and actual
 352 sowing dates. It must also be considered that the GGCMI crop calendar is based on statistics that apply to discrete areas
 353 at relatively coarse half degree spatial resolution, while CropSuite was simulated at a pixel accuracy of 30 arc seconds
 354 spatial resolution. In fact, the median differences are mostly within one month of the GGCMI crop calendar, which
 355 generally indicates a high agreement. At the coarse resolution, the difference between the two datasets is less and the
 356 spread is smaller (Fig. S5).
 357



358
 359 **Figure 9: Comparison of the optimal sowing dates of CropSuite with the actual sowing dates of the GGCMI crop calendars.**
 360 The area-weighted shift of the sowing date in days is shown for all matching crops. Negative values mean an earlier sowing date in
 361 CropSuite, positive values mean a later sowing date in CropSuite compared to the GGCMI Crop Calendar. The bars show the 5th and
 362 95th percentile, the orange marker shows the median. The color of the bars indicates the climatically suitable area for the whole of
 363 Africa. Irrigated areas are considered according to Meier et al. (2018). The comparison is performed at 30 arc seconds spatial resolution
 364 for both datasets.

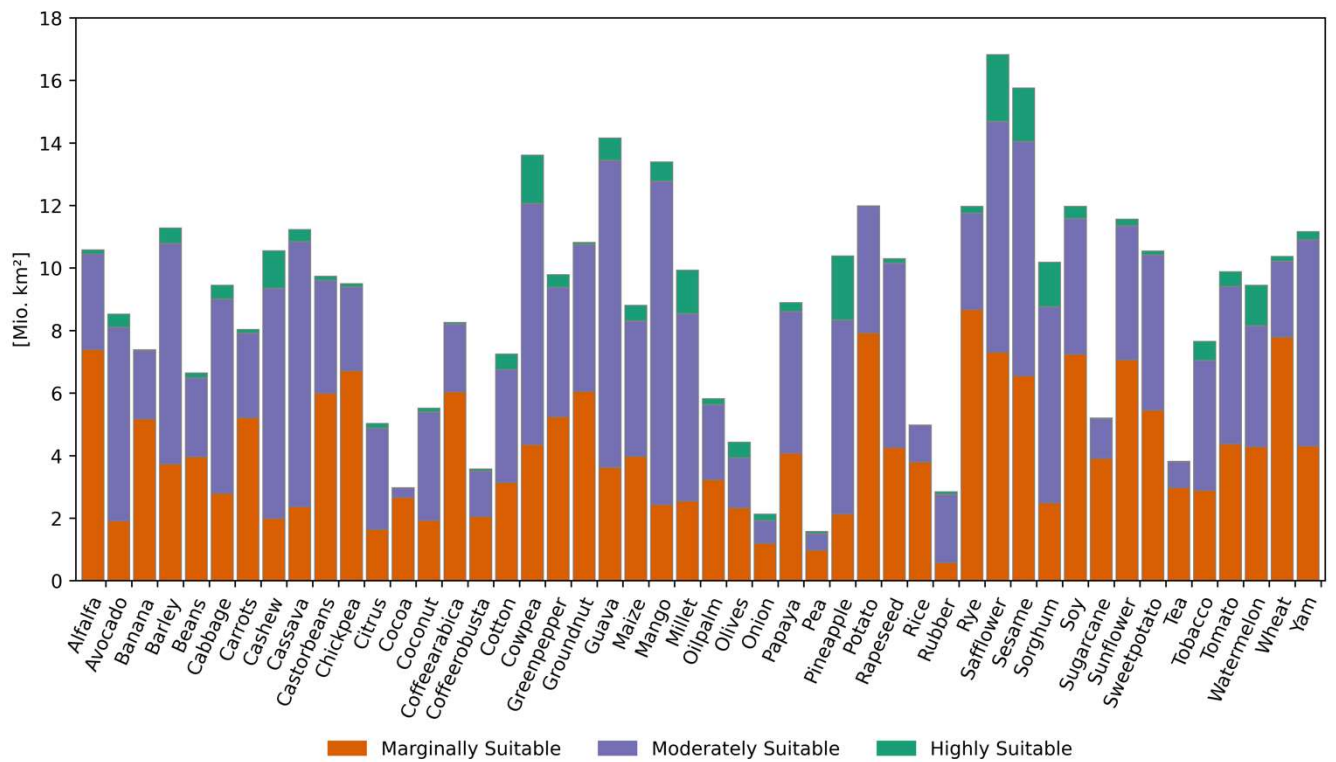
365 **4 Simulation Results**

366 Crop suitability is simulated for historical climate conditions (1991-2010) for rainfed and irrigated conditions. Figure 10a
367 illustrates the overall crop suitability, showing for each location the value for the most suitable of all considered crops.
368 Irrigation is considered according to the currently irrigated areas for Africa (Meier et al., 2018), such as along the Nile
369 river in Egypt (see Fig. S1 for irrigated areas in Africa). In total for Africa, 5.7 million km² are highly suitable, 10.6
370 million km² are moderately suitable, 3.3 million km² are marginally suitable and 10.4 million km² are not suitable for
371 crop cultivation. Mainly between 10° N and 10° S, a high potential for multiple cropping exists with the possibility of
372 two or three harvests per year (Fig. 10b). Looking at the number of crops suitable for cultivation (Fig. 10c), a large
373 proportion of the considered crops can grow particularly along the wet savannahs, which gives these regions plenty of
374 opportunities for cultivation. In contrast, only a few crops are suitable for the inner tropics and the dry savannahs, which
375 limits the possibilities for switching between culturescrops.



376
377 **Figure 10: (a) Overall crop suitability, (b) potential multiple cropping, and (c) number of suitable crops under historical climate**
378 **conditions from 1991 to 2010.** Irrigated areas are considered according to Meier et al. (2018). The overall crop suitability (a) and the
379 potential multiple cropping (b) are each shown for the most suitable crop at each location. The maximal number of suitable crops
380 results from the number of 48 considered crops (see Table 1).

381 Figure 11 shows the suitable area for each of the simulated crops for Africa. The five crops with the largest suitable areas
382 in Africa are safflower (16.82 mio km²), sesame (15.76), guava (14.15), cowpea (13.61), and mango (13.39).



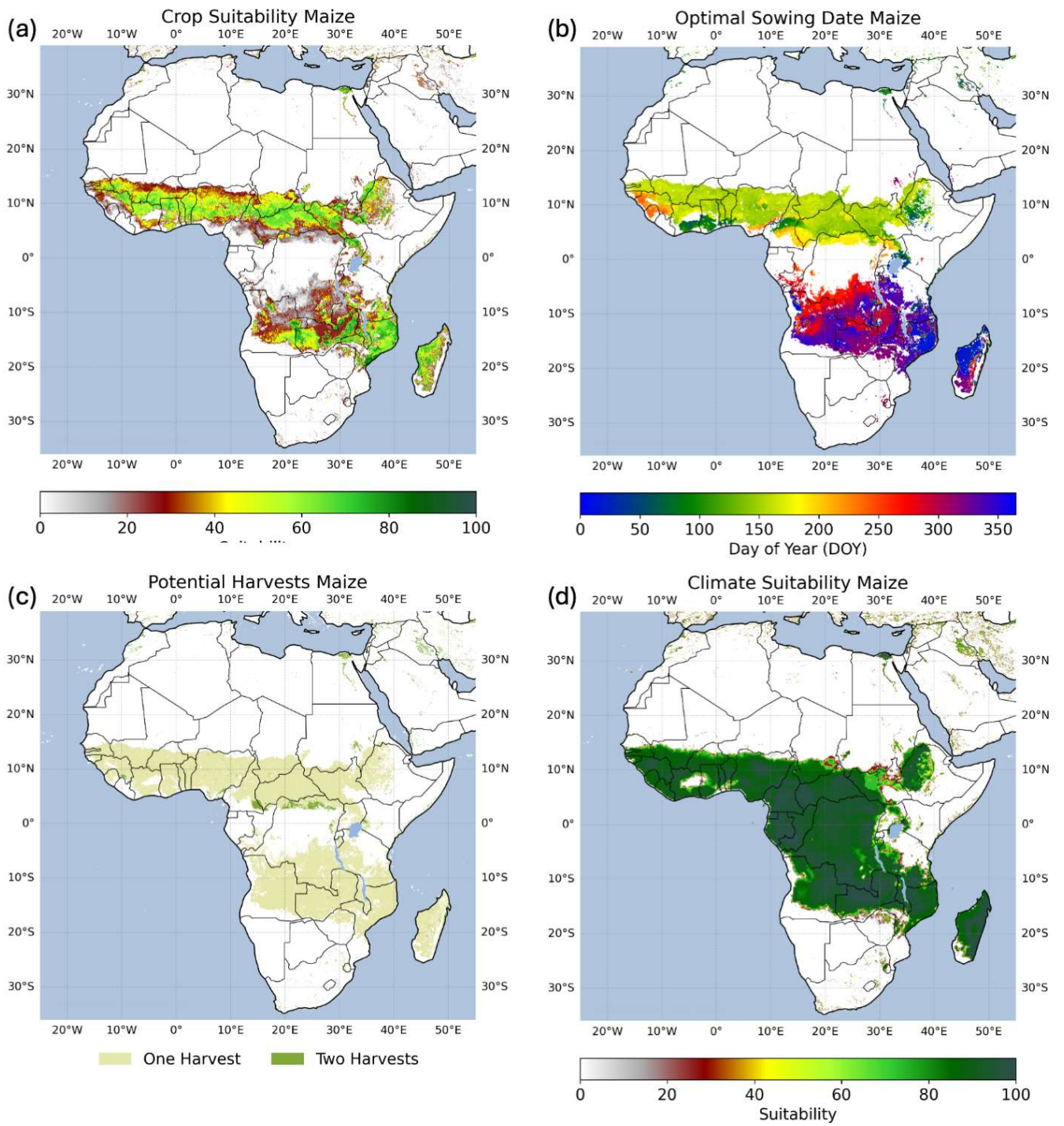
383

384 **Figure 11: Marginally, moderately and highly suitable areas for all 48 crops under historical climate conditions from 1991 to**
 385 **2010 for Africa.** Suitability classes are chosen according to Table 3. Irrigated areas are considered according to Meier et al. (2018).

386 Figure 12a exemplarily shows the crop suitability simulated for maize. The maps for all crops are provided via Zenodo
 387 (see Data Availability). Maize is highly suitable along a strip of the 10° N and the 20° S parallel as well as large parts of
 388 Mozambique and Madagascar. In total, 0.49 million km² are highly suitable, 4.34 million km² are moderately suitable,
 389 3.97 million km² are marginally suitable and 21.23 million km² are unsuitable.

390 The optimal sowing date for single cropping (Fig. 12b) for maize shifts with latitude from the northern hemisphere across
 391 the equator to the southern hemisphere. Figure 12c shows the potential number of potential harvests per year for maize.
 392 Climate conditions allow up to two harvests per year in some parts of Congo and Cameroon and in the irrigated areas e.g.
 393 along the Nile river. Optimal sowing dates for first and second sowing on areas suitable for multiple cropping are shown
 394 in Fig. S26.

395 Figure 12d shows the climate suitability for maize, which just considers climatic constraints for the suitability of maize.
 396 In comparison to the crop suitability [map](#) (Fig. 12a), more areas are suitable and suitability is substantially higher, **where**
 397 **[if](#) soil and topography [are not considered and therefore](#) do not limit or reduce crop suitability.**



398

399

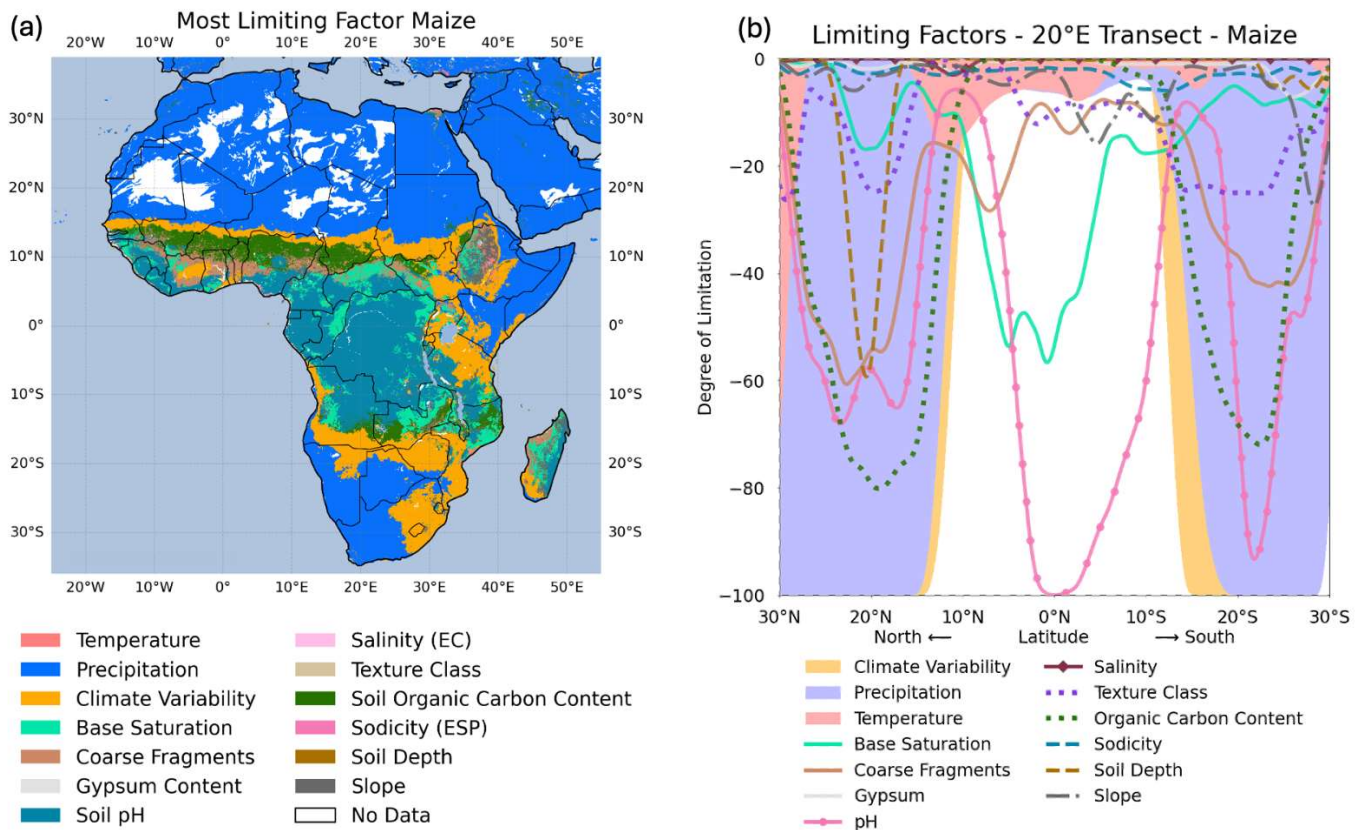
400

401

Figure 12: (a) Crop suitability, (b) optimal sowing date for single cropping, (c) potential multiple cropping, and (d) climate suitability for maize under historical climate conditions from 1991 to 2010. Irrigated areas are considered according to Meier et al. (2018).

402 The most limiting factor is shown in Fig. 13a. While low precipitation prevents maize from being suitable in large parts
403 of Africa in the arid deserts, soil is predominantly restricting suitability in tropical regions. Particularly pH is the most
404 limiting factor in the humid tropics, such as the Congo Basin, where soils are too acid for growing maize. A large band
405 along the drylands highlights regions where inter-annual climate variability is most limiting maize suitability (in orange,
406 Fig. 13a). Here, climate conditions are unstable for maize cultivation, and the recurrence rate of potential crop failures is
407 larger than 25% (every fourth year). For maize, climate variability is limiting crop suitability on 4.4 million km² for
408 Africa (Fig 13a).

409 Figure 13b shows the degree of limitation for all considered climate, soil and terrain factors along a transect following
410 the 20° E from North to South. In the Sahara, several factors, including temperature, organic carbon content, and soil pH,
411 are not in an optimal range, while precipitation and the climate variability are the most limiting (note that climate
412 variability is by definition a limiting factor if precipitation and/or temperature are limiting factors). Due to the unfavorable
413 soil conditions, irrigation would only slightly improve maize suitability here. Between 15° N and 5° N, the limitations of
414 all factors are relatively low. Here, coarse fragments and base saturation are most limiting. The tropical areas along the
415 transect between 5° N and 10° S are mainly constrained by soil pH. Accordingly, soil management or practices that
416 increase pH in these regions would have a significantly positive impact on crop suitability in this region, since no other
417 factor has such a strong impact on maize suitability. Further south, low precipitation again mostly limits maize suitability.



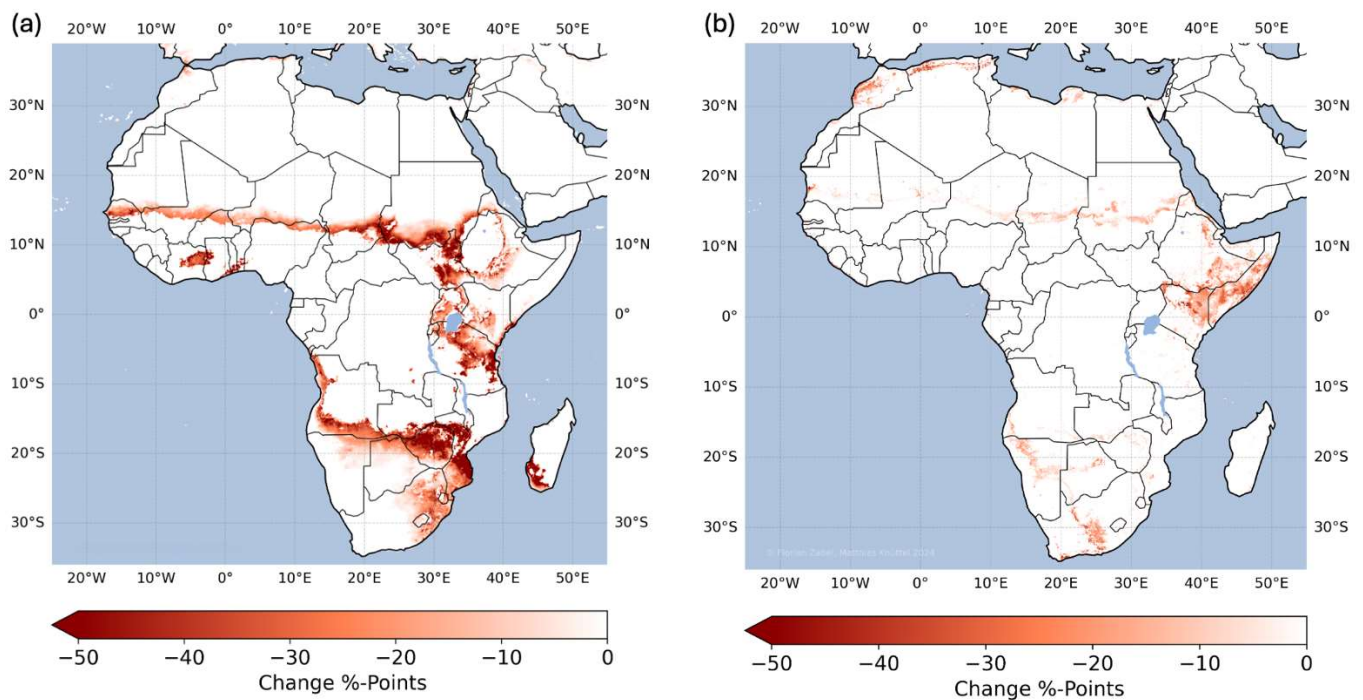
418

419 **Figure 13: Limiting factors.** (a) Most limiting factor of the crop suitability for maize under historical climate conditions from 1991
 420 to 2010. (b) shows the degree of limitation of all factors along a transect of the 20° East from 30° North to 30° South. The most limiting
 421 factors are displayed with priority according to the order in the legend in (a), if more than one factor fully limits the suitability. For
 422 visualization, the shapes in (b) are smoothed using a moving average. Irrigated areas are considered according to Meier et al. (2018)
 423 in (a) and are not considered in (b).

424 The consideration of climate variability significantly reduces climate suitability for maize as shown in Fig. 14a, mainly
 425 in the transition area between dry savannah and desert in the Sahel zone, in Burundi and Tanzania in Eastern Africa, and
 426 in the southern part of Africa in Angola, Zambia, Zimbabwe, Mozambique, South Africa, and the southern part of
 427 Madagascar. In total, climate variability reduces climate suitability on more than 5.4 million km².

428 Optimal sowing dates also shift when considering climate variability, since the algorithm identifies the best suitable time
 429 window for the growing cycle over the year (Fig. S37). As a result, optimal sowing for maize considerably shifts in
 430 Tanzania, Mozambique and Madagascar.

431 Over all crops, Fig. 14b shows the impact of climate variability on the overall crop suitability. In this case, overall crop
 432 suitability is reduced on 2.2 million km², mainly reduced in Somalia, Kenya, Ethiopia, South Africa, and the Maghreb
 433 countries of Morocco, Algeria, Tunisia, and Libya. These regions generally show a high vulnerability to climatic
 434 variability. Climate variability also reduces the potential for multiple cropping in general over all crops on more than 2.3
 435 million km² (Fig. S48).



436

437

438

Figure 14: Impact of the consideration of climate variability on crop suitability (a) for maize (b) for the overall crop suitability of all crops under historical climate conditions from 1991 to 2010. Irrigated areas are considered according to Meier et al. (2018).

439

5 Discussion

440

We found that the consideration of climate variability significantly affects crop suitability, multiple cropping, and optimal sowing dates in Africa. Our approach allows to adjust the risk aversion of farmers by adjusting the thresholds for climate variability (section 2.2.) and the membership function (Fig. 5). The shape of this function may differ between crops and regions and might be influenced by several socio-economic factors, such as the degree of mechanization, financial possibilities, and the availability of crop insurances, which is likely to reduce risk aversion of farmers. We suggest the function as shown in Fig. 5 as a broad and general solution which is primarily designed to represent risk aversion of commercial farms. In our comparison analysis for maize (section 3), reference data showed some cultivation, ~~we were able to determine that still agriculture takes place~~ in the regions we identified as unsuitable due to the high recurrence rate of potential crop failures caused by high climate variability (Fig. 7). In some regions, despite the high risk of crop failures, land might be cultivated by smallholders or subsistence farmers that have no other choice but to cultivate these lands. ~~Though~~ ~~However~~, we admit that the tuning of the climate variability thresholds and the membership function requires more research, and the optimal results will vary depending on crop and region. ~~However~~, CropSuite offers the platform and the possibilities to conduct such assessments.

452

453 The results of CropSuite ([section 4](#)) are subject to uncertainties in the applied climate, soil, terrain, and irrigation data as
454 well as the membership functions ([Fig. 1](#)). Soil and terrain data are assumed to be static, although management could
455 influence soil properties, such as pH, and terracing could reduce slope limitations. [The applied climate data from CHIRPS
456 and CHIRTS are found to be particularly valuable in regions, where climate stations are sparse. Over Africa, CHIRPS is
457 successfully validated \(Dinku et al., 2018\) showing good performance \(Lemma et al., 2019; Muthoni et al., 2019\).](#) Verdin
458 et al. (2020) [also report good agreement of CHIRTS over Africa, however with a poor performance over central Africa,
459 the Horn of Africa, and parts of northern Mali. Generally, both data sets rely on station data to correct the satellite
460 estimations, which is why uncertainties for very data-scarce regions remain. To apply CropSuite in regions outside 50°S-
461 50°N, or to larger time periods before the 1980s, the user of CropSuite could also rely on global high-resolution climate
462 reanalysis, such as ERA5 \(Hersbach et al., 2020\). For the African continent, Even though ERA5 reanalysis shows large
463 improvements over its predecessor ERA-Interim for the African continent \(Gleixner et al., 2020\).](#) Still, considerable
464 [deviations in precipitation from CHIRPS biases remain are reported, e.g., wet biases over Uganda \(Gleixner et al., 2020\)
465 and ai \(Steinkopf and Engelbrecht, 2022; Terblanche et al., 2022\) dry bias over the western Sahel \(Gbode et al., 2023\),
466 where CHIRPS is applied as reference. We therefore assume that CHIRPS and CHIRTS are very suitable climatic data
467 sets to investigate our example of maize suitability in Africa.](#) The soil profiles used for the generation of the SoilGrids
468 show a heterogeneous distribution, with large gaps over central Africa, which is why Hengl et al. (2017) attribute
469 uncertainty in the data to the under-sampling. They argue that a few hundred additional profiles in under-sampled areas
470 could massively improve the resulting SoilGrids.

471 The membership functions derived by Sys et al. (1993) are widely applied but are also governed by inherent uncertainties.
472 Herzberg et al. (2019) argue that the assessment by Sys et al. (1993) is not detailed enough to capture specific features of
473 small areas. They find that Sys et al. (1993) would consider a hilly area in tropical Vietnam unsuitable due to too acidic
474 soils and steep slopes, whereas the local farmers can cultivate the land. Furthermore, the approach cannot account for
475 compound effects and interactions of the climate and soil variables (Elsheikh et al., 2013). The membership functions
476 cover the general behavior in a univariate manner, while the real plant physiology is a more complex interplay of climatic
477 variables and soil conditions (Joswig et al., 2022). This also applies particularly to compound extremes, for example the
478 combination of hot and dry climatic conditions (Goulart et al., 2023) that limit water availability and favor evaporation,
479 which can trigger water and temperature stress in plants. This is relevant in the course of a warming climate, as the joint
480 probability of hot and dry conditions is projected to increase in many regions of the world (Bevacqua et al., 2022; Felsche
481 et al., 2024). This is however no specific drawback of CropSuite, but rather a lack of bivariate, multivariate or interactive
482 membership functions. The assessment [of the membership functions](#) by Sys et al. (1993) is also outdated for new crop
483 varieties that might be more resilient to climatic and environmental stressors (Peter et al., 2020). Furthermore, we argue
484 that the uncertainty in the [temperature and precipitation](#) membership functions is by design larger at ~~the~~ its low and high
485 ends, [as the functions are derived empirically. Since of the membership function, which affect](#) our consideration of
486 climate variability [is based on the 5% to 10% suitability values, respectively \(see Section 2.2\), the uncertainties of the](#)

487 [membership functions are propagated to the assessment of climate variability](#). More research and updated functions could
488 support the results by CropSuite.

489 The sampling of climate variability within 20-year periods is limited as variability can cover wide time ranges. There,
490 the application of single-model initial condition large ensembles can help to robustly assess the variability based on
491 decadal or multidecadal time periods (Deser et al., 2020). This is especially important for precipitation and precipitation
492 extremes, which show a high sensitivity to climate variability (Lang and Poschlod, 2024; Tebaldi et al., 2021).
493 Furthermore, for the assessment of climate variability, we only capture the occurrence of growing seasons exceeding the
494 percentile thresholds, but we do not consider the intensity of the according events. Single days with extreme precipitation
495 can induce flooding that leads to crop failures (Balgah et al., 2023; Müller et al., 2023), even though the average
496 precipitation for the growing season is still within the suitable range of the membership function. This drawback however
497 also applies for [most of the](#) mechanistic crop models [at global scale](#) (Ruane et al., 2017), [while regional applications](#)
498 [evolve incorporating crop losses due to waterlogging and flooding](#) (Li et al., 2016; Monteleone et al., 2023; Pasley et al.,
499 2020). This is why we claim to assess climate variability not climate extremes inducing potential crop failures.

500 **6 Conclusions**

501 CropSuite is a new easy-to-use comprehensive open-source model that provides a complete processing chain
502 (preprocessing, spatial downscaling, suitability simulations, data analysis and visualization) for carrying out crop
503 suitability and climate change impact analysis. CropSuite allows users to easily parameterize different varieties of the
504 same crops or additional crops by determining the membership functions in the GUI. Thereby, the fuzzy logic approach
505 makes it easy to use expert knowledge for the parameterization of the membership functions. Besides all data and
506 compiled maps generated, we provide a user manual for CropSuite (Zabel and Knüttel, 2024) and the parameterizations
507 of the considered 48 crops in this study. Furthermore, the model allows the flexible addition of further parameters and
508 membership functions that might affect suitability, if the required data is provided. For the future, this allows the
509 consideration of further ecological and socio-economic limitations (such as access to fertilizers, available labor, know-
510 how, infrastructure and transportation, heat stress impacts on labor) that have not yet been sufficiently considered in
511 crop suitability assessments (Orlov et al., 2024; Akpoti et al., 2019).

512 For this study, we simulated 48 crops for Africa under the consideration of climate variability for historical climate
513 conditions. Thus, we created a huge dataset, providing detailed high-resolution information on climate-, soil-, and crop
514 suitability, optimal sowing dates, multiple cropping potentials and the limiting factors, which can be used for follow-up
515 studies and climate impact assessments. Additionally, the data include substantial information to develop strategies for
516 an efficient land-use (Schneider et al., 2024; Molina Bacca et al., 2023; Delzeit et al., 2019). The consideration of future
517 climate change scenarios will allow for investigating efficient strategies for climate change adaptation through shifting

518 sowing dates, or cultivar and land-use change. Further, information about the limiting factors can be helpful to optimize
519 crop management, since it identifies the parameter that most efficiently improves crop suitability.

520 **Code Availability**

521 CropSuite (v01.90) code is written in Python and is available Open-Source (CC BY-SA 4.0) together with the GUI and
522 a user manual at Zenodo (<https://doi.org/10.5281/zenodo.14259375>) and GitHub
523 (<https://github.com/flozabel/CropSuite>). A user manual is provided separately via Zenodo
524 (<https://doi.org/10.5281/zenodo.14196315>).

525 **Data Availability**

526 The resulting data are available for download as GeoTIFF files ~~seen~~ via Zenodo
527 (<https://doi.org/10.5281/zenodo.14196331>). (~~https://adaptationatlas.cgiar.org~~). In addition to the ~~shown~~ figures shown as
528 examples for maize in this paper, the compiled figures for all 48 considered crops are provided for download, including
529 a separation of rainfed and irrigated agricultural systems and a comparison with MapSPAM 2020
530 (<https://doi.org/10.5281/zenodo.14196331>).

531 **Author contribution**

532 FZ conceptualized and developed the model. MK programmed the CropSuite model and the GUI in Python. FZ, MK,
533 and BP developed the methodology for the consideration of climate variability. FZ and MK performed the simulations
534 and analyzed the results. FZ and MK prepared the manuscript with contributions from BP.

535 **Competing interests**

536 The authors declare that they have no conflict of interest.

537 **Acknowledgements**

538 The simulations were performed at sciCORE (<http://scicore.unibas.ch/>) scientific computing center at University of
539 Basel, requiring in total approximately 150.000 CPUh. We thank CGIAR and CIAT for their support and the scholarship
540 provided to MK and the collaboration for the Africa Agriculture Adaptation Atlas.

- 542 Abdulai, A. L., Kouressy, M., Vaksman, M., Asch, F., Giese, M., and Holger, B.: Latitude and Date of Sowing
543 Influences Phenology of Photoperiod-Sensitive Sorghums, *Journal of Agronomy and Crop Science*, 198, 340-348,
544 10.1111/j.1439-037X.2012.00523.x, 2012.
- 545 Akpoti, K., Kabo-bah, A. T., and Zwart, S. J.: Review - Agricultural land suitability analysis: State-of-the-art and outlooks
546 for integration of climate change analysis, *Agricultural Systems*, 173, 172-208,
547 <https://doi.org/10.1016/j.agsy.2019.02.013>, 2019.
- 548 Akpoti, K., Kabo-bah, A. T., Dossou-Yovo, E. R., Groen, T. A., and Zwart, S. J.: Mapping suitability for rice production
549 in inland valley landscapes in Benin and Togo using environmental niche modeling, *Science of The Total*
550 *Environment*, 709, 136165, <https://doi.org/10.1016/j.scitotenv.2019.136165>, 2020.
- 551 Asseng, S., Spänkuch, D., Hernandez-Ochoa, I. M., and Laporta, J.: The upper temperature thresholds of life, *The Lancet*
552 *Planetary Health*, 5, e378-e385, [https://doi.org/10.1016/S2542-5196\(21\)00079-6](https://doi.org/10.1016/S2542-5196(21)00079-6), 2021.
- 553 Avellan, T., Zabel, F., and Mauser, W.: The influence of input data quality in determining areas suitable for crop growth
554 at the global scale – a comparative analysis of two soil and climate datasets, *Soil Use and Management*, 28, 249-265,
555 <https://doi.org/10.1111/j.1475-2743.2012.00400.x>, 2012.
- 556 Balgah, R. A., Ngwa, K. A., Buchenrieder, G. R., and Kimengsi, J. N.: Impacts of Floods on Agriculture-Dependent
557 Livelihoods in Sub-Saharan Africa: An Assessment from Multiple Geo-Ecological Zones, *Land*, 12, 334, 2023.
- 558 Batjes, N. H.: Harmonized soil property values for broad-scale modelling (WISE30sec) with estimates of global soil
559 carbon stocks, *Geoderma*, 269, 61-68, <https://doi.org/10.1016/j.geoderma.2016.01.034>, 2016.
- 560 Bevacqua, E., Zappa, G., Lehner, F., and Zscheischler, J.: Precipitation trends determine future occurrences of compound
561 hot–dry events, *Nat Clim Change*, 12, 350-355, 10.1038/s41558-022-01309-5, 2022.
- 562 Bonfante, A., Monaco, E., Alfieri, S. M., De Lorenzi, F., Manna, P., Basile, A., and Bouma, J.: Chapter Two - Climate
563 Change Effects on the Suitability of an Agricultural Area to Maize Cultivation: Application of a New Hybrid Land
564 Evaluation System, in: *Advances in Agronomy*, edited by: Sparks, D. L., Academic Press, 33-69,
565 <https://doi.org/10.1016/bs.agron.2015.05.001>, 2015.
- 566 Chapman, S., E Birch, C., Pope, E., Sallu, S., Bradshaw, C., Davie, J., and H Marsham, J.: Impact of climate change on
567 crop suitability in sub-Saharan Africa in parameterized and convection-permitting regional climate models,
568 *Environmental Research Letters*, 15, 094086, 10.1088/1748-9326/ab9daf, 2020.
- 569 Chemura, A., Gleixner, S., and Gornott, C.: Dataset of the suitability of major food crops in Africa under climate change,
570 *Scientific Data*, 11, 294, 10.1038/s41597-024-03118-1, 2024.
- 571 Chen, D., Dai, A., and Hall, A.: The Convective-To-Total Precipitation Ratio and the “Drizzling” Bias in Climate Models,
572 *Journal of Geophysical Research: Atmospheres*, 126, e2020JD034198, <https://doi.org/10.1029/2020JD034198>, 2021.
- 573 Cober, E. R. and Morrison, M. J.: Regulation of seed yield and agronomic characters by photoperiod sensitivity and
574 growth habit genes in soybean, *Theoretical and Applied Genetics*, 120, 1005-1012, 10.1007/s00122-009-1228-6,
575 2010.
- 576 Cronin, J., Zabel, F., Dessens, O., and Anandarajah, G.: Land suitability for energy crops under scenarios of climate
577 change and land-use, *GCB Bioenergy*, 12, 648–665-648–665, <https://doi.org/10.1111/gcbb.12697>, 2020.
- 578 Daly, C., Neilson, R. P., and Phillips, D. L.: A Statistical-Topographic Model for Mapping Climatological Precipitation
579 over Mountainous Terrain, *Journal of Applied Meteorology and Climatology*, 33, 140-158,
580 [https://doi.org/10.1175/1520-0450\(1994\)033<0140:ASTMFM>2.0.CO;2](https://doi.org/10.1175/1520-0450(1994)033<0140:ASTMFM>2.0.CO;2), 1994.
- 581 Damiani, A., Ishizaki, N. N., Sasaki, H., Feron, S., and Cordero, R. R.: Exploring super-resolution spatial downscaling
582 of several meteorological variables and potential applications for photovoltaic power, *Scientific Reports*, 14, 7254,
583 10.1038/s41598-024-57759-8, 2024.
- 584 Delzeit, R., Pongratz, J., Schneider, J. M., Schuenemann, F., Mauser, W., and Zabel, F.: Forest restoration: Expanding
585 agriculture, *Science*, 366, 316–317-316–317, <https://doi.org/10.1126/science.aaz0705>, 2019.
- 586 Deser, C., Lehner, F., Rodgers, K. B., Ault, T., Delworth, T. L., DiNezio, P. N., Fiore, A., Frankignoul, C., Fyfe, J. C.,
587 Horton, D. E., Kay, J. E., Knutti, R., Lovenduski, N. S., Marotzke, J., McKinnon, K. A., Minobe, S., Randerson, J.,
588 Screen, J. A., Simpson, I. R., and Ting, M.: Insights from Earth system model initial-condition large ensembles and
589 future prospects, *Nat Clim Change*, 10, 277-286, 10.1038/s41558-020-0731-2, 2020.

- 590 Dinku, T., Funk, C., Peterson, P., Maidment, R., Tadesse, T., Gadain, H., and Ceccato, P.: Validation of the CHIRPS
591 satellite rainfall estimates over eastern Africa, *Quarterly Journal of the Royal Meteorological Society*, 144, 292-312,
592 <https://doi.org/10.1002/qj.3244>, 2018.
- 593 Elsheikh, R., Mohamed Shariff, A. R. B., Amiri, F., Ahmad, N. B., Balasundram, S. K., and Soom, M. A. M.: Agriculture
594 Land Suitability Evaluator (ALSE): A decision and planning support tool for tropical and subtropical crops, *Comput
595 Electron Agr*, 93, 98-110, <https://doi.org/10.1016/j.compag.2013.02.003>, 2013.
- 596 FAO: The Ecocrop Database [dataset], 2024.
- 597 FAO, IIASA, ISRIC, ISSCAS, and JRC: Harmonized World Soil Database (version 1.2) [dataset], 2012.
- 598 Farr, T. G., Rosen, P. A., Caro, E., Crippen, R., Duren, R., Hensley, S., Kobrick, M., Paller, M., Rodriguez, E., Roth, L.,
599 Seal, D., Shaffer, S., Shimada, J., Umland, J., Werner, M., Oskin, M., Burbank, D., and Alsdorf, D.: The Shuttle
600 Radar Topography Mission, *Reviews of Geophysics*, 45, RG2004, 10.1029/2005RG000183, 2007.
- 601 Felsche, E., Böhnisch, A., Poschlod, B., and Ludwig, R.: European hot and dry summers are projected to become more
602 frequent and expand northwards, *Communications Earth & Environment*, 5, 410, 10.1038/s43247-024-01575-5,
603 2024.
- 604 Fick, S. E. and Hijmans, R. J.: WorldClim 2: new 1-km spatial resolution climate surfaces for global land areas,
605 *International Journal of Climatology*, 37, 4302-4315, 10.1002/joc.5086, 2017.
- 606 Fiddes, J., Aalstad, K., and Lehning, M.: TopoCLIM: rapid topography-based downscaling of regional climate model
607 output in complex terrain v1.1, *Geosci. Model Dev.*, 15, 1753-1768, 10.5194/gmd-15-1753-2022, 2022.
- 608 Fischer, G., Nachtergaele, F. O., van Velthuizen, H. T., Chiozza, F., Franceschini, G., Henry, M., Muchoney, D., and
609 Tramberend, S.: Global Agro-Ecological Zones v4 - Model documentation, 1, FAO, Rome,
610 <https://doi.org/10.4060/cb4744en>, 2021.
- 611 Franke, J. A., Müller, C., Minoli, S., Elliott, J., Folberth, C., Gardner, C., Hank, T., Izaurrealde, R. C., Jägermeyr, J., Jones,
612 C. D., Liu, W., Olin, S., Pugh, T. A. M., Ruane, A. C., Stephens, H., Zabel, F., and Moyer, E. J.: Agricultural
613 breadbaskets shift poleward given adaptive farmer behavior under climate change, *Global Change Biol*, 28, 167-181-
614 167-181, <https://doi.org/10.1111/gcb.15868>, 2021.
- 615 Funk, C., Peterson, P., Landsfeld, M., Pedreros, D., Verdin, J., Shukla, S., Husak, G., Rowland, J., Harrison, L., Hoell,
616 A., and Michaelsen, J.: The climate hazards infrared precipitation with stations—a new environmental record for
617 monitoring extremes, *Scientific Data*, 2, 150066, 10.1038/sdata.2015.66, 2015.
- 618 Funk, C., Peterson, P., Peterson, S., Shukla, S., Davenport, F., Michaelsen, J., Knapp, K. R., Landsfeld, M., Husak, G.,
619 Harrison, L., Rowland, J., Budde, M., Meiburg, A., Dinku, T., Pedreros, D., and Mata, N.: A High-Resolution 1983–
620 2016 Tmax Climate Data Record Based on Infrared Temperatures and Stations by the Climate Hazard Center, *Journal
621 of Climate*, 32, 5639-5658, <https://doi.org/10.1175/JCLI-D-18-0698.1>, 2019.
- 622 Gbode, I. E., Babalola, T. E., Diro, G. T., and Intsiful, J. D.: Assessment of ERA5 and ERA-Interim in Reproducing
623 Mean and Extreme Climates over West Africa, *Advances in Atmospheric Sciences*, 40, 570-586, 10.1007/s00376-
624 022-2161-8, 2023.
- 625 Gleixner, S., Demissie, T., and Diro, G. T.: Did ERA5 Improve Temperature and Precipitation Reanalysis over East
626 Africa?, *Atmosphere*, 11, 996, 2020.
- 627 Goulart, H. M. D., van der Wiel, K., Folberth, C., Balkovic, J., and van den Hurk, B.: Storylines of weather-induced crop
628 failure events under climate change, *Earth Syst. Dynam.*, 12, 1503-1527, 10.5194/esd-12-1503-2021, 2021.
- 629 Goulart, H. M. D., van der Wiel, K., Folberth, C., Boere, E., and van den Hurk, B.: Increase of Simultaneous Soybean
630 Failures Due To Climate Change, *Earth's Future*, 11, e2022EF003106, <https://doi.org/10.1029/2022EF003106>, 2023.
- 631 Hengl, T., de Jesus, J. M., MacMillan, R. A., Batjes, N. H., Heuvelink, G. B. M., Ribeiro, E., Samuel-Rosa, A., Kempen,
632 B., Leenaars, J. G. B., Walsh, M. G., and Gonzalez, M. R.: SoilGrids1km — Global Soil Information Based on
633 Automated Mapping, *PLOS ONE*, 9, e105992, 10.1371/journal.pone.0105992, 2014.
- 634 Hengl, T., Mendes de Jesus, J., Heuvelink, G. B. M., Ruiperez Gonzalez, M., Kilibarda, M., Blagotić, A., Shangguan,
635 W., Wright, M. N., Geng, X., Bauer-Marschallinger, B., Guevara, M. A., Vargas, R., MacMillan, R. A., Batjes, N.
636 H., Leenaars, J. G. B., Ribeiro, E., Wheeler, I., Mantel, S., and Kempen, B.: SoilGrids250m: Global gridded soil
637 information based on machine learning, *PLOS ONE*, 12, e0169748, 10.1371/journal.pone.0169748, 2017.
- 638 Hersbach, H., Bell, B., Berrisford, P., Hirahara, S., Horányi, A., Muñoz-Sabater, J., Nicolas, J., Peubey, C., Radu, R.,
639 Schepers, D., Simmons, A., Soci, C., Abdalla, S., Abellan, X., Balsamo, G., Bechtold, P., Biavati, G., Bidlot, J.,

640 Bonavita, M., De Chiara, G., Dahlgren, P., Dee, D., Diamantakis, M., Dragani, R., Flemming, J., Forbes, R., Fuentes,
641 M., Geer, A., Haimberger, L., Healy, S., Hogan, R. J., Hólm, E., Janisková, M., Keeley, S., Laloyaux, P., Lopez, P.,
642 Lupu, C., Radnoti, G., de Rosnay, P., Rozum, I., Vamborg, F., Villaume, S., and Thépaut, J.-N.: The ERA5 global
643 reanalysis, *Quarterly Journal of the Royal Meteorological Society*, 146, 1999-2049, <https://doi.org/10.1002/qj.3803>,
644 2020.

645 Herzberg, R., Pham, T. G., Kappas, M., Wyss, D., and Tran, C. T. M.: Multi-Criteria Decision Analysis for the Land
646 Evaluation of Potential Agricultural Land Use Types in a Hilly Area of Central Vietnam, *Land*, 8, 90, 2019.

647 IFPRI: Global Spatially-Disaggregated Crop Production Statistics Data for 2020 Version 1.0, Harvard Dataverse
648 [dataset], <https://doi.org/10.7910/DVN/SWPENT>, 2024.

649 IPCC: Climate Change 2021: The Physical Science Basis. Contribution of Working Group I to the Sixth Assessment
650 Report of the Intergovernmental Panel on Climate Change, Cambridge University Press, 2021.

651 Ivushkin, K., Bartholomeus, H., Bregt, A. K., Pulatov, A., Kempen, B., and de Sousa, L.: Global mapping of soil salinity
652 change, *Remote Sens Environ*, 231, 111260, <https://doi.org/10.1016/j.rse.2019.111260>, 2019.

653 Jägermeyr, J., Robock, A., Elliott, J., Müller, C., Xia, L., Khabarov, N., Folberth, C., Schmid, E., Liu, W., Zabel, F.,
654 Rabin, S. S., Puma, M. J., Heslin, A., Franke, J., Foster, I., Asseng, S., Bardeen, C. G., Toon, O. B., and Rosenzweig,
655 C.: A regional nuclear conflict would compromise global food security, *Proceedings of the National Academy of
656 Sciences*, 117, 7071–7081-7071–7081, <https://doi.org/10.1073/pnas.1919049117>, 2020.

657 Jägermeyr, J., Müller, C., Ruane, A. C., Elliott, J., Balkovic, J., Castillo, O., Faye, B., Foster, I., Folberth, C., Franke, J.
658 A., Fuchs, K., Guarin, J. R., Heinke, J., Hoogenboom, G., Iizumi, T., Jain, A. K., Kelly, D., Khabarov, N., Lange, S.,
659 Lin, T.-S., Liu, W., Mialyk, O., Minoli, S., Moyer, E. J., Okada, M., Phillips, M., Porter, C., Rabin, S. S., Scheer, C.,
660 Schneider, J. M., Schyns, J. F., Skalsky, R., Smerald, A., Stella, T., Stephens, H., Webber, H., Zabel, F., and
661 Rosenzweig, C.: Climate impacts on global agriculture emerge earlier in new generation of climate and crop models,
662 *Nature Food*, 2, 873–885-873–885, <https://doi.org/10.1038/s43016-021-00400-y>, 2021.

663 Joswig, J. S., Wirth, C., Schuman, M. C., Kattge, J., Reu, B., Wright, I. J., Sippel, S. D., Rüger, N., Richter, R.,
664 Schaepman, M. E., van Bodegom, P. M., Cornelissen, J. H. C., Diaz, S., Hattigh, W. N., Kramer, K., Lens, F.,
665 Niinemets, Ü., Reich, P. B., Reichstein, M., Römermann, C., Schrodt, F., Anand, M., Bahn, M., Byun, C., Campetella,
666 G., Cerabolini, B. E. L., Craine, J. M., Gonzalez-Melo, A., Gutiérrez, A. G., He, T., Higuchi, P., Jactel, H., Kraft, N.
667 J. B., Minden, V., Onipchenko, V., Peñuelas, J., Pillar, V. D., Sosinski, Ê., Soudzilovskaia, N. A., Weiher, E., and
668 Mahecha, M. D.: Climatic and soil factors explain the two-dimensional spectrum of global plant trait variation, *Nature
669 Ecology & Evolution*, 6, 36-50, 10.1038/s41559-021-01616-8, 2022.

670 Karger, D. N., Lange, S., Hari, C., Reyer, C. P. O., Conrad, O., Zimmermann, N. E., and Frieler, K.: CHELSA-W5E5:
671 daily 1 km meteorological forcing data for climate impact studies, *Earth Syst. Sci. Data*, 15, 2445-2464,
672 10.5194/essd-15-2445-2023, 2023.

673 Karl, K., MacCarthy, D., Porciello, J., Chimwaza, G., Fredenberg, E., Freduah, B. S., Guarin, J., Mendez Leal, E.,
674 Kozłowski, N., Narh, S., Sheikh, H., Valdivia, R., Wesley, G., Van Deynze, A., van Zonneveld, M., and Yang, M.:
675 Opportunity Crop Profiles for the Vision for Adapted Crops and Soils (VACS) in Africa,
676 <https://doi.org/10.7916/7msa-yy32>, 2024.

677 Knüttel, M. and Zabel, F.: CropSuite User Manual, <https://doi.org/10.5281/zenodo.14196315>, 2024.

678 Lang, A. and Poschlo, B.: Updating catastrophe models to today's climate – An application of a large ensemble approach
679 to extreme rainfall, *Climate Risk Management*, 44, 100594, <https://doi.org/10.1016/j.crm.2024.100594>, 2024.

680 Lemma, E., Upadhyaya, S., and Ramsankaran, R.: Investigating the performance of satellite and reanalysis rainfall
681 products at monthly timescales across different rainfall regimes of Ethiopia, *International Journal of Remote Sensing*,
682 40, 4019-4042, 10.1080/01431161.2018.1558373, 2019.

683 Li, S., Tompkins, A. M., Lin, E., and Ju, H.: Simulating the impact of flooding on wheat yield – Case study in East China,
684 *Agr Forest Meteorol*, 216, 221-231, <https://doi.org/10.1016/j.agrformet.2015.10.014>, 2016.

685 Maleki, F., Kazemi, H., Siahmarguee, A., and Kamkar, B.: Development of a land use suitability model for saffron
686 (*Crocus sativus* L.) cultivation by multi-criteria evaluation and spatial analysis, *Ecol Eng*, 106, 140-153,
687 <https://doi.org/10.1016/j.ecoleng.2017.05.050>, 2017.

688 Marke, T., Mauser, W., Pfeiffer, A., Zängl, G., Jacob, D., and Strasser, U.: Application of a hydrometeorological model
689 chain to investigate the effect of global boundaries and downscaling on simulated river discharge, *Environ Earth Sci*,
690 71, 4849-4868, 10.1007/s12665-013-2876-z, 2014.

691 Meier, J., Zabel, F., and Mauser, W.: A global approach to estimate irrigated areas – a comparison between different data
692 and statistics, *Hydrology and Earth System Sciences*, 22, 1119–1133-1119–1133, 2018.

693 Molina Bacca, E. J., Stevanović, M., Bodirsky, B. L., Karstens, K., Chen, D. M.-C., Leip, D., Müller, C., Minoli, S.,
694 Heinke, J., Jägermeyr, J., Folberth, C., Iizumi, T., Jain, A. K., Liu, W., Okada, M., Smerald, A., Zabel, F., Lotze-
695 Campen, H., and Popp, A.: Uncertainty in land-use adaptation persists despite crop model projections showing lower
696 impacts under high warming, *Communications Earth & Environment*, 4, 284, 10.1038/s43247-023-00941-z, 2023.

697 Monteleone, B., Giusti, R., Magnini, A., Arosio, M., Domeneghetti, A., Borzi, I., Petruccelli, N., Castellarin, A.,
698 Bonaccorso, B., and Martina, M. L. V.: Estimations of Crop Losses Due to Flood Using Multiple Sources of
699 Information and Models: The Case Study of the Panaro River, *Water*, 15, 1980, 2023.

700 Müller, C., Ouédraogo, W. A., Schwarz, M., Barteit, S., and Sauerborn, R.: The effects of climate change-induced
701 flooding on harvest failure in Burkina Faso: case study, *Frontiers in Public Health*, 11, 10.3389/fpubh.2023.1166913,
702 2023.

703 Müller, C., Jägermeyr, J., Franke, J. A., Ruane, A. C., Balkovic, J., Ciais, P., Dury, M., Falloon, P., Folberth, C., Hank,
704 T., Hoffmann, M., Izaurrealde, R. C., Jacquemin, I., Khabarov, N., Liu, W., Olin, S., Pugh, T. A. M., Wang, X.,
705 Williams, K., Zabel, F., and Elliott, J. W.: Substantial Differences in Crop Yield Sensitivities Between Models Call
706 for Functionality-Based Model Evaluation, *Earth's Future*, 12, e2023EF003773,
707 <https://doi.org/10.1029/2023EF003773>, 2024.

708 Muthoni, F. K., Odongo, V. O., Ochieng, J., Mugalavai, E. M., Mourice, S. K., Hoesche-Zeledon, I., Mwila, M., and
709 Bekunda, M.: Long-term spatial-temporal trends and variability of rainfall over Eastern and Southern Africa,
710 *Theoretical and Applied Climatology*, 137, 1869-1882, 10.1007/s00704-018-2712-1, 2019.

711 Orlov, A., Jägermeyr, J., Müller, C., Daloz, A. S., Zabel, F., Minoli, S., Liu, W., Lin, T.-S., Jain, A. K., Folberth, C.,
712 Okada, M., Poschlod, B., Smerald, A., Schneider, J. M., and Sillmann, J.: Human heat stress could offset potential
713 economic benefits of CO2 fertilization in crop production under a high-emissions scenario, *One Earth*, 7, 1250-1265,
714 <https://doi.org/10.1016/j.oneear.2024.06.012>, 2024.

715 Pasley, H. R., Huber, I., Castellano, M. J., and Archontoulis, S. V.: Modeling Flood-Induced Stress in Soybeans, *Frontiers*
716 *in Plant Science*, 11, 10.3389/fpls.2020.00062, 2020.

717 Pelletier, J. D., Broxton, P. D., Hazenberg, P., Zeng, X., Troch, P. A., Niu, G.-Y., Williams, Z., Brunke, M. A., and
718 Gochis, D.: A gridded global data set of soil, intact regolith, and sedimentary deposit thicknesses for regional and
719 global land surface modeling, *Journal of Advances in Modeling Earth Systems*, 8, 41-65,
720 <https://doi.org/10.1002/2015MS000526>, 2016.

721 Peter, B. G., Messina, J. P., Lin, Z., and Snapp, S. S.: Crop climate suitability mapping on the cloud: a geovisualization
722 application for sustainable agriculture, *Scientific Reports*, 10, 15487, 10.1038/s41598-020-72384-x, 2020.

723 Ramirez-Villegas, J., Jarvis, A., and Läderach, P.: Empirical approaches for assessing impacts of climate change on
724 agriculture: The EcoCrop model and a case study with grain sorghum, *Agr Forest Meteorol*, 170, 67-78,
725 <https://doi.org/10.1016/j.agrformet.2011.09.005>, 2013.

726 Ranjitkar, S., Sujakhu, N. M., Merz, J., Kindt, R., Xu, J., Matin, M. A., Ali, M., and Zomer, R. J.: Suitability Analysis
727 and Projected Climate Change Impact on Banana and Coffee Production Zones in Nepal, *PLOS ONE*, 11, e0163916,
728 10.1371/journal.pone.0163916, 2016.

729 Ruane, A. C., Rosenzweig, C., Asseng, S., Boote, K. J., Elliott, J., Ewert, F., Jones, J. W., Martre, P., McDermid, S. P.,
730 Müller, C., Snyder, A., and Thorburn, P. J.: An AgMIP framework for improved agricultural representation in
731 integrated assessment models, *Environmental Research Letters*, 12, 125003, 10.1088/1748-9326/aa8da6, 2017.

732 Schneider, J. M., Zabel, F., and Mauser, W.: Global inventory of suitable, cultivable and available cropland under
733 different scenarios and policies, *Scientific Data*, 9, <https://doi.org/10.1038/s41597-022-01632-8>, 2022a.

734 Schneider, J. M., Zabel, F., and Mauser, W.: Global inventory of suitable, cultivable and available cropland under
735 different scenarios and policies, *Scientific Data*, 9, 527, 10.1038/s41597-022-01632-8, 2022b.

736 Schneider, J. M., Delzeit, R., Neumann, C., Heimann, T., Seppelt, R., Schuenemann, F., Söder, M., Mauser, W., and
737 Zabel, F.: Effects of profit-driven cropland expansion and conservation policies, *Nature Sustainability*, 7, 1335-1347,
738 10.1038/s41893-024-01410-x, 2024.

739 Steinkopf, J. and Engelbrecht, F.: Verification of ERA5 and ERA-Interim precipitation over Africa at intra-annual and
740 interannual timescales, *Atmospheric Research*, 280, 106427, <https://doi.org/10.1016/j.atmosres.2022.106427>, 2022.

741 Sun, Y., Solomon, S., Dai, A., and Portmann, R. W.: How Often Does It Rain?, *Journal of Climate*, 19, 916-934,
742 10.1175/jcli3672.1, 2006.

743 Sys, C. O., van Ranst, E., and Debaveye, J.: Land evaluation: Part II Methods in Land Evaluation, G.A.D.C, Brussels,
744 1991.

745 Sys, C. O., van Ranst, E., Debaveye, J., and Beernaert, F.: Land evaluation: Part III Crop requirements, G.A.D.C,
746 Brussels, 1993.

747 Tebaldi, C., Dorheim, K., Wehner, M., and Leung, R.: Extreme metrics from large ensembles: investigating the effects
748 of ensemble size on their estimates, *Earth Syst. Dynam.*, 12, 1427-1501, 10.5194/esd-12-1427-2021, 2021.

749 Terblanche, D., Lynch, A., Chen, Z., and Sinclair, S.: ERA5-Derived Precipitation: Insights from Historical Rainfall
750 Networks in Southern Africa, *Journal of Applied Meteorology and Climatology*, 61, 1473-1484,
751 <https://doi.org/10.1175/JAMC-D-21-0096.1>, 2022.

752 van Zonneveld, M., Kindt, R., McMullin, S., Achigan-Dako, E. G., N'Danikou, S., Hsieh, W.-h., Lin, Y.-r., and Dawson,
753 I. K.: Forgotten food crops in sub-Saharan Africa for healthy diets in a changing climate, *Proceedings of the National
754 Academy of Sciences*, 120, e2205794120, 10.1073/pnas.2205794120, 2023.

755 Verdin, A., Funk, C., Peterson, P., Landsfeld, M., Tuholske, C., and Grace, K.: Development and validation of the
756 CHIRTS-daily quasi-global high-resolution daily temperature data set, *Scientific Data*, 7, 303, 10.1038/s41597-020-
757 00643-7, 2020.

758 Vogel, E., Donat, M. G., Alexander, L. V., Meinshausen, M., Ray, D. K., Karoly, D., Meinshausen, N., and Frieler, K.:
759 The effects of climate extremes on global agricultural yields, *Environmental Research Letters*, 14, 054010,
760 10.1088/1748-9326/ab154b, 2019.

761 Wang, F., Tian, D., Lowe, L., Kalin, L., and Lehrter, J.: Deep Learning for Daily Precipitation and Temperature
762 Downscaling, *Water Resources Research*, 57, e2020WR029308, <https://doi.org/10.1029/2020WR029308>, 2021.

763 Yu, Q., You, L., Wood-Sichra, U., Ru, Y., Joglekar, A. K. B., Fritz, S., Xiong, W., Lu, M., Wu, W., and Yang, P.: A
764 cultivated planet in 2100 – Part 2: The global gridded agricultural-production maps, *Earth Syst. Sci. Data*, 12, 3545-
765 3572, 10.5194/essd-12-3545-2020, 2020.

766 Zabel, F.: Global Agricultural Land Resources – A High Resolution Suitability Evaluation and Its Perspectives until 2100
767 under Climate Change Conditions (v3.0) Zenodo [dataset], <https://doi.org/10.5281/zenodo.5982577>, 2022.

768 Zabel, F. and Knüttel, M.: CropSuite Version 1.0 User Manual, 21.05.2024.

769 Zabel, F., Putzenlechner, B., and Mauser, W.: Global Agricultural Land Resources – A High Resolution Suitability
770 Evaluation and Its Perspectives until 2100 under Climate Change Conditions, *PLoS ONE*, 9, e107522-e107522,
771 <https://doi.org/10.1371/journal.pone.0107522>, 2014.

772